TROPICAL AND EXTRA-TROPICAL AIR-SEA INTERACTIONS

Edited by Swadhin K. Behera

Chapter 7

The Atlantic zonal mode: dynamics, thermodynamics, and tele-connections

INGO RICHTER[1]

[1]*Application Laboratory, Research Institute for Value-Added-Information Generation, Japan Agency for Marine-Earth Science and Technology, Yokohama, Japan*

HIROKI TOKINAGA[2]

[2]*Research Institute for Applied Mechanics, Kyushu University, Kasuga, Japan*

submitted, 1 August 2019

revised, 24 January 2020

accepted, 31 January 2020

Corresponding author address:

Ingo Richter

Application Laboratory, JAMSTEC, 3173-25 Showa-machi, Kanazawa-ku, Yokohama, Kanagawa 236-0001, Japan

E-mail: richter@jamstec.go.jp

ABSTRACT

The equatorial Atlantic is subject to variability on interannual timescales that involves coupled air-sea interaction and bears some similarity to the El Niño-Southern Oscillation (ENSO) in the tropical Pacific. In this chapter we take a closer look at equatorial Atlantic variability, examining its dynamical and thermodynamical mechanisms, its interaction with other variability patterns inside and outside the tropical Atlantic, its influences on precipitation over land, its representation in climate models, its predictability, and its low-frequency modulation. In addition to reviewing what is known about the equatorial Atlantic, we also point out where there is a current lack of consensus and where there are open questions requiring further research.

1. Introduction

The equatorial Atlantic is subject to sea-surface temperature (SST) variations that are most pronounced in the eastern and central part of the basin and occur on interannual time-scales. These variations are tightly locked to the annual cycle and have their peak in boreal summer, with a secondary peak in boreal fall (e.g. Lübbecke et al. 2018; Fig. 14). Historically, this pattern of variability was discovered after El Niño-Southern Oscillation (ENSO) came to prominence, with first observational evidence emerging in the 1970s and 1980s (Hastentrath and Heller 1977; Katz et al. 1977; Merle 1980; Hisard 1980). Those observations suggested a certain similarity to the ENSO phenomenon in the Pacific, including (for the positive phase) a weakening of the equatorial trades, weakening of the south-equatorial current, strengthening of the north-equatorial counter current and equatorial undercurrent, and deepening of the equatorial thermocline. Due to these similarities, Hisard (1980) described the phenomenon as the Atlantic counterpart to El Niño, and the term "Atlantic Niño" gradually gained currency in the literature. Subsequent studies identified differences between equatorial variability in the Atlantic and Pacific (Zebiak 1993; Keenlyside and Latif 2007; Foltz and McPhaden 2010a; Burls et al. 2012; Richter et al. 2013; Nnamchi et al. 2015). In recognition of these differences the term "Atlantic zonal mode" (AZM) is now increasingly being used in the literature, and we will follow this terminology.

Compared to ENSO, the AZM has a relatively small SST amplitude of about 1 K. Nevertheless, AZM events have been associated with far reaching impacts, including European winter weather (Ventzke et al. 1999; Rodwell et al. 1999; Scaife et al. 2017) the tropical Pacific (Rodriguez-Fonseca et al. 2009), and the Indian summer monsoon (Pottapinjara et al. 2014, 2016; Kucharski et al. 2016).

In this chapter, we will give an overview of the current understanding of equatorial Atlantic variability. Recently, several reviews on the topic have been published, with one focusing on equatorial Atlantic variability alone (Lübbecke et al. 2018) and two discussing it as part of their description of the tropical Atlantic observation network (Bourles et al. 2019; Foltz et al. 2019). In difference to those reviews, here we will focus more narrowly on the mechanisms of equatorial Atlantic variability, which allows us to go into some more detail. Based on recently published data sets, we will also present some new analysis that hopefully may serve as a reference for future research. Being the work of only two authors, this chapter will certainly be biased toward the authors' own research findings, though we will strive to give a relatively comprehensive overview, present a spectrum of opinions and point to controversies and unsolved questions.

The data sets and some definitions are briefly described in section 2. In section 3 we present the climatological annual cycle of the equatorial Atlantic, which will be needed for a deeper understanding of its interannual variability. Section 4 explains the dynamical and thermodynamical mechanisms underlying equatorial Atlantic variability. The linkage of the AZM to other tropical Atlantic patterns of variability is described in section 5. The influence of the AZM on the surrounding continents, and its two-way interactions with remote basins are the topic of section 6. The extent to which numerical models can simulate and predict equatorial Atlantic variability is examined in sections 7 and 8, respectively. In section 9, we take a brief look at low-frequency modulation and long-term trends in the equatorial Atlantic. The final section 10 presents a summary of this chapter and outlines some outstanding research questions and conundrums.

2. Data description and definition

Most of the analysis presented here is based on the European Centre for Medium Range Weather Forecasting (ECMWF) reanalysis 5 (ERA5; Hersbach et al. 2018), and on the ECMWF Ocean Reanalysis 4 (ORAS4; Balmaseda et al. 2013), both for the period 1979-2018. Precipitation data is from the Global Precipitation Climatology Project (GPCP) version 2.3 (Adler et al. 2018). The NCEP/NCAR reanalysis (Kalnay et al. 1996) is used to present a longer time series of equatorial Atlantic SST variability (1948-2018). To illustrate the performance of global climate models (GCMs), we use an ensemble of simulations from the preindustrial control experiment (piControl) of the Coupled Model Intercomparison Project phase 5 (CMIP5). These simulations were performed as part of the Intergovernmental Panel on Climate Change (IPCC) 5th Assessment Report (AR5). The ensemble consists of the following members: ACCESS1-0, ACCESS1-3, bcc-csm1-1, BNU-ESM, CanESM2, CCSM4, CSIRO-Mk3-6-0, EC-EARTH, FGOALS-g2, FGOALS-s2, FIO-ESM, GFDL-CM3, GFDL-ESM2G, GFDL-ESM2M, GISS-E2-H, GISS-E2-R, HadGEM2-ES, inmcm4, MIROC4h, MIROC5, MIROC-ESM, MPI-ESM-LR, and MPI-ESM-MR.

Several averaging areas are used to describe the climate and variability of the tropics. These are summarized in Table 1.

The following abbreviations are used to denote seasonal averages: MAM (March-May), JJA (June-August), SON (September-October), and DJF (December-February).

3. Climatological annual cycle of the equatorial Atlantic

The equatorial Atlantic is subject to a pronounced annual cycle. In March and April, SSTs tend to be uniformly warm across the equatorial basin while the intertropical convergence zone (ITCZ) attains its southernmost position, right over the equator, and the equatorial trades are at their weakest (Fig. 1). From April through August, SST in the eastern equatorial Atlantic (measured here by the ATL3 index, Table 1) drop from 28.7ºC to 24.4ºC (Fig. 2). In the western and central equatorial Atlantic (as measured by the ATL4 index, Table 1), SSTs decrease as well over this period but at a slower rate, resulting in a noticeable zonal SST gradient along the equator in boreal summer (Fig. 1). The relatively cool summer SSTs that extend from the African coast to about 20ºW are usually referred to as the Atlantic cold tongue. Its development is closely linked to the strengthening of the equatorial trades (Fig. 1), which drive cooling both through local Ekman divergence (Busalacchi and Picaut 1983; Foltz et al. 2003) and through shoaling of the thermocline induced by Kelvin waves forced in the western equatorial Atlantic (Moore et al. 1978; Adamec and O'Brien 1978; Busalacchi and Picaut 1983; McCreary et al. 1984). A further contribution comes from the annual cycle of surface net shortwave radiation (Foltz et al. 2003).

The strength of the equatorial trades is linked to the latitudinal position of the ITCZ (Fig. 3; Richter et al. 2014a), which moves from about 0.5ºN in March to 9ºN in August. The ITCZ represents the convergence of the southeast and northeast trade wind systems and thus a shift in its latitude is expected to modulate the strength of the trades at any given location. This relation, however, can be complicated by other factors, such as horizontal and vertical momentum transport, and this appears to be the case over the equatorial Atlantic, as will be discussed in section 4.

It is of interest that, during boreal spring, the equatorial Atlantic zonal sea-level pressure (SLP) gradient is directed *eastward* from about 35ºW to the coast (Fig. 4). If the pressure gradient force were the sole driver of surface zonal winds, westerlies should prevail. Observations, however, show easterlies almost all the way to the eastern boundary (Fig. 4). Thus, other processes must maintain the easterly surface winds. Based on a simple momentum budget analysis, Richter et al. (2014b) conclude that horizontal momentum transport is insufficient to provide the missing source of easterly momentum, leaving vertical momentum transport as the most likely candidate. This is supported by the fact that, in spring, deep convection is present over the equator, and that horizontal momentum is well mixed in the lower troposphere (Richter et al. 2014b).

The vertical sections along the equator of atmospheric and oceanic fields (Fig. 5) give an impression of the large-scale circulation changes that occur from MAM to JJA. The trade wind strengthening from April through August has a clear effect on the equatorial thermocline (and, more evidently, on the 23ºC isotherm), whose zonal slope steepens. The atmospheric Walker circulation also undergoes profound changes between MAM and JJA, with subsidence strengthening over the eastern equatorial Atlantic and ascent weakening over the western equatorial Atlantic and South America. This, again, is linked to the northward shift of the ITCZ (Fig. 1), which is associated with the end of the rainy season over the Nordeste region on one side and the beginning of the West African monsoon on the other.

An interesting detail to note in Fig. 1 is the lack of collocation between maximum SST and precipitation. In MAM, for example, maximum precipitation is located right over the equator while the maximum SST is centered on 5ºS. The reason for this behavior has not

been fully explained but it may be related to the strong precipitation maximum over equatorial South America.

Figure 2 shows that, from July to September, the surface zonal winds are weakening, before strengthening again until November. This behavior is particularly pronounced in the eastern equatorial Atlantic, where it is accompanied by a secondary shoaling of the thermocline in November (Okumura and Xie 2006). The timing of the climatological thermocline shoaling is closely related to the phasing of equatorial Atlantic variability patterns as will be explained in the following section.

4. Dynamical and thermodynamical elements of equatorial Atlantic variability

4.1. Introduction

Interannual variability in the equatorial Atlantic displays some similarity to that in the equatorial Pacific. This includes SST anomalies in the central equatorial basin that are preceded by a weakening of the equatorial trades and a deepening of the equatorial thermocline. It is also thought that the Bjerknes feedback[1] plays a crucial role in both basins (Zebiak 1993; Keenlyside and Latif 2007; Dippe and Greatbatch 2017; Lübbecke and McPhaden 2013, 2017). In difference to ENSO, however, the AZM preferentially occurs in boreal summer, is shorter lived and of weaker amplitude.

[1] An air-sea coupled feedback on the equator, first hypothesized by Bjerknes (1969), in which initial SST anomalies, induce surface wind anomalies that change the thermocline depth and reinforce the initial SST anomalies. See chapter 3 on ENSO, or Keenlyside and Latif (2007).

Figure 6 shows the ATL3 time series from 1949-2018. Interannual variability is evident in Fig. 6 but also extended warm and cold periods during which multiple peaks of the same sign occur. Previous studies have shown that the ATL3 spectrum is generally red, with weak peaks in the 1.5 to 4 year band (Zebiak 1993; Latif and Grötzner 2000; Ruiz-Barradas et al. 2000; Tseng and Mechoso 2001). The most pronounced warm event in the 70-year record appears to have occurred in 1963, followed by the most pronounced cold event in late 1964. There is a general impression that variability has weakened in recent decades, which will be briefly discussed in section 9.

4.2. Composite evolution of the AZM

The composite evolution of a positive AZM event (Atlantic Niño) is shown in Fig. 7. As early as February there are weak warm SST anomalies on the equator and along the southwest African coast, the latter being indicative of a Benguela Niño (see Chapter 10 of this volume). At the same time, northwesterly surface wind anomalies can be seen over the western equatorial Atlantic and, indeed, over the entire southern tropical Atlantic. In March, a more coherent pattern emerges, with surface wind and SST anomalies intensifying on the equator, accompanied by positive rainfall anomalies. The wind and precipitation anomalies continue to grow in April and peak in May. In terms of horizontal distribution, there is a clear east-west asymmetry with wind and precipitation anomalies strongest in the west, and SST anomalies strongest in the east. The SST anomalies reach their peak one month later, in June, when wind and precipitation anomalies are already subsiding. In July, SST anomalies on the equator are decaying but remain quite strong in the southeastern tropical Atlantic. Throughout the evolution, precipitation anomalies are most pronounced over the ocean but there are wet anomalies over equatorial South America from March through July and along the Guinea coast in June and July.

The vertical sections of ocean temperature (Fig. 9) show how warm anomalies at the depth of the thermocline are already present in February. As cool anomalies develop in the west during the following months, the warm anomalies become confined to the east. The accompanying thermocline anomalies, while relatively subtle, indicate a shoaling of the thermocline. Both the surface and subsurface warm anomalies peak in June. One month later, the subsurface anomalies are much weaker, while the surface anomalies are only slightly weakened. The sequence of events suggests that the climatological upwelling that picks up in May brings the subsurface anomalies to the surface but also gradually erodes the surface warm anomalies once the event runs out of fuel (i.e. wind stress forcing and downwelling Kelvin waves).

The vertical atmospheric sections (Fig. 9) show that convective anomalies in May and June are strongest at 30ºW and to the west, which is consistent with the precipitation anomalies (Fig. 7). This may first seem surprising, as the SST anomalies are stronger to the east, but can be explained by the evolving background state (Fig. 1). Closer inspection of climatological SSTs in May and June (not shown though inferable from Fig. 2) indicates that, due to the incipient cold tongue formation, SSTs in the eastern equatorial Atlantic drop well below 27ºC while at 30ºW they are around 27.5ºC, close to the deep convective threshold. This is likely one of the reasons why deep convection occurs there, though other factors may contribute.

4.3. Phase locking

An interesting detail in Fig. 9 concerns the zonal wind anomalies in the lower troposphere. While the anomalies at the surface peak in May, those at 700 hPa are actually stronger in June and July, consistent with the maximum anomalous SST and sea-level pressure gradients during these months. Richter et al. (2017) argue that the northward shift of

the ITCZ in June and July is responsible for this behavior. They hypothesize that, as the ITCZ moves northward, vertical momentum transport on the equator decreases due to the decline of convective activity, allowing for momentum anomalies to grow in the lower troposphere, above the surface. Irrespective of the mechanism, it is evident that the northward migration of the ITCZ is closely linked to the decline of equatorial surface wind anomalies (Figs. 3 and 11 in Richter et al. 2017; also Fig. 7), which in turn leads to the demise of AZM events.

Thus, evidence seems to suggest that the seasonal migration of the ITCZ is a key element to the phase locking of AZM events to boreal summer. Other studies have argued for the seasonal shoaling of the thermocline to be an important factor for invigorating the Bjerknes feedback and thus allowing for the growth of SST anomalies (Okumura and Xie 2006; Keenlyside et al. 2007; for the Pacific: Battisti and Hirst 1989; Philander et al. 1996; Jin 1997). This argument certainly has merit too but cannot explain why events often decay in July and August, when the thermocline is still shallow. Martin-Rey et al. (2019) note that positive (negative) AZM events are often accompanied by wind stress curl anomalies just north of the equator that excite upwelling (downwelling) Rossby waves. These are subsequently reflected into equatorial Kelvin waves at the western boundary and can thus influence the equator. A similar mechanism has been described to explain other aspects of equatorial Atlantic variability (see subsection 4.6). Martin-Rey et al. (2019) argue that these Kelvin waves are crucial to the decay of AZM events as they counteract the original SST anomalies. Their analysis, however, seems to suggest that the reflected Kelvin waves do not reach the ATL3 region until August or September, when the decay is already well underway. More detailed case studies will be necessary to quantify the importance of this

mechanism. It should also be noted that the mechanism proposed by Richter et al. (2017), struggles to explain the seasonality of the Atlantic Niño II (section 4.5), as the ITCZ is off the equator during both development and decay of this variability pattern.

4.4. Negative AZM events - symmetry

The composites of negative AZM events (Figs. 8 and 10) suggest they evolve analogously to positive ones, though the former appear to decline more rapidly in July. Lübbecke and McPhaden (2017) performed a detailed observational analysis of negative and positive AZM events and found that they are essential mirror images of each other with respect to amplitude, location, and temporal evolution, consistent with the impression from our composites. Analyzing an oceanic GCM (OGCM) forced with CORE2 surface fluxes, Jouanno et al. (2017) obtained similar results but found that the damping effect of horizontal advection is somewhat more pronounced during warm events.

4.5. Atlantic Niño II

As noted in section 3, in boreal fall there is a secondary strengthening of the equatorial trades (Fig. 2) and shoaling of the thermocline. Okumura and Xie (2006) show that this secondary shoaling is associated with equatorial Atlantic SST variability that peaks in November and December and named it Atlantic Niño II (AN2). AN2 shows no significant correlations to either the AZM or ENSO (Okumura and Xie 2006). Like the AZM, it appears to rely on the Bjerknes feedback. Its amplitude is only about half as strong as that of the AZM, but may contribute to rainfall anomalies over Africa and also contribute to the development of the tropical Atlantic meridional mode, to be described in section 5.

4.6. Non-canonical AZM events

The analogy between the AZM and ENSO has often been emphasized (e.g. Lübbecke and McPhaden 2017). The evolution of ENSO, in its developing phase, crucially depends

on wind stress anomalies over the western and central equatorial Pacific, the so-called westerly wind bursts and easterly wind surges (e.g. Harrison and Vecchi 1997; Eisenman et al. 2005). These wind events force equatorial Kelvin waves that influence thermocline depth and SSTs to the east. Thus, there is a strong link between anomalous wind stress and SST. This is clearly seen in a scatter plot of JJA wind vs. DJF SST anomalies (Fig. 11a; also, Richter et al. 2013). Richter et al. (2013) found that such a clear relation is lacking in the equatorial Atlantic. In fact, westerly wind events can be followed by *cool* SST anomalies and vice versa (Fig. 11b). Richter et al. (2013) termed these events non-canonical, to distinguish them from the regular (or canonical) AZM. They suggested, based on an OGCM forced with NCEP/NCAR reanalysis surface forcing, that non-canonical events develop due to meridional temperature advection in the subsurface ocean. They show that non-canonical warm events are typically preceded by trade wind weakening and SST warming in the northern tropical Atlantic, accompanied by easterly surface wind anomalies on the equator (Fig. 11b). This configuration leads to wind stress curl anomalies just north of the equator that induce downward Ekman pumping and subsurface warming. As a result, warm ocean anomalies form just north of the equator, which can be advected into the equatorial region by the mean circulation. These subsurface anomalies then warm the SST through upwelling and vertical mixing. Once an initial SST warming has occurred, it can be amplified by the Bjerknes feedback. Several other studies have analyzed this phenomenon but have arrived at a different conclusion regarding the mechanism underlying non-canonical AZM events (Foltz et al. 2010a; Lübbecke and McPhaden 2012; Burmeister et al. 2016). While those authors agree on the importance of wind stress curl anomalies, they

suggest that these excite off-equatorial downwelling Rossby waves, which are subsequently reflected into downwelling equatorial Kelvin waves at the western boundary. A heat budget analysis by Burmeister et al. (2016) suggests that most non-canonical events are due to the Rossby wave mechanism, though there may be an additional role for meridional advection in a few cases. Richter et al. (2013), on the other hand, point out that wave reflection at the western boundary is difficult to detect in observations and that it may occur too late to have a significant influence. More detailed analysis will be required to arrive at a consensus. See also the discussion by Lübbecke (2013).

4.7. Thermodynamic AZM

While ocean dynamics have long been regarded as central to the understanding of ENSO (e.g. Jin 1997; Neelin et al. 1998), a few recent studies have challenged this notion (Clement et al. 2011; Zhang et al. 2014) by suggesting that thermodynamic processes can explain some portion of ENSO variability. In a similar vein, Nnamchi et al. (2015, 2016) suggested that the Atlantic Niño can be largely explained by thermodynamic processes. This was mainly based on an analysis of atmospheric GCMs coupled to a slab ocean (slab ocean control experiment in the CMIP3 archive). Despite the absence of ocean dynamics, these models produce similar patterns as their fully coupled GCM (CGCM) counterparts at about 2/3 of the amplitude. Nnamchi et al. (2015) suggest that solar radiation and latent heat flux are the crucial components in the development of slab-ocean AZM events. Inspection of the early stages of positive AZM events (Fig. 7) does indeed show that weakening of the trade winds is not confined to the equator but covers most of the southern tropical Atlantic. This is indicative of a weakening of the St. Helena high, as noted by several authors (Lübbecke et al. 2010; Richter et al. 2010; Nnamchi et al. 2015; Richter and Doi 2019). Such a weakening of the southeast trades leads to reduced latent heat flux

and anomalous SST warming. Two subsequent studies (Dippe et al. 2017; Jouanno et al. 2017) have questioned the dominance of thermodynamical processes in AZM events on the grounds that these results were mainly obtained from model simulations, which are subject to severe biases (e.g. Richter et al. 2014a). These studies argue that the unrealistically deep equatorial thermocline in biased model simulations render the Bjerknes feedback ineffective, leading to equatorial variability that is dominated by thermodynamic processes. The notion that thermodynamic processes dominate equatorial Atlantic variability is also at odds with several observation-based studies of the ocean heat budget during AZM events (Ding et al. 2010; Planton et al. 2018). On the other hand, turbulent heat fluxes are difficult to measure, as are terms in the ocean heat budget. Thus, while ocean dynamics should not be discounted on account of the work of Nnamchi et al. (2015, 2016), these results do point to a need for a better understanding of the role of thermodynamic process in AZM events.

4.8. Initiation of AZM events

The temporal evolution of AZM events suggests that equatorial wind stress forcing in early spring is key to their development. During this time, SST anomalies tend to be weak (Fig. 7), raising the question of the origin of wind anomalies. Richter et al. (2014a) show that there is a high correlation between the strength of equatorial surface wind anomalies and the latitude of the Atlantic ITCZ: the further south the ITCZ moves, the weaker the equatorial winds become (Fig. 12). This relation, which also holds for the climatological annual cycle (Fig. 2), is not only remarkable for its strength (correlation coefficient ~ 0.8) but also for its asymmetry with respect to the equator. While the reason for this asymmetry remains largely unexplored, it is known that the ITCZ position is subject to off-equatorial influences (Kang et al. 2008; Frierson and Hwang 2012), and that it may be influenced

from remote basins (Giannini et al. 2001; Sasaki et al. 2015). This allows other variability patterns to link to the AZM.

While coupled air-sea processes undoubtedly are important to the AZM, Richter et al. (2014a) and Richter and Doi (2019) argue that internal atmospheric variability also plays a significant role. Using an atmospheric GCM (AGCM) forced with the observed climatological annual cycle of SST (i.e. no SST anomalies anywhere), Richter and Doi (2019) show that anomalous wind events still preferentially occur in MAM though the amplitude is about one fourth of that of the control experiment with observed SST. The equatorial wind anomalies are part of a much larger pattern that, for westerly wind events, includes a southward shift of the Atlantic ITCZ, weakening of the St. Helena high, strengthening of the Azores high, and high pressure anomalies over the eastern equatorial Pacific. While such anomalies can be the seed for AZM events, it is clear that coupled feedbacks, in particular the Bjerknes feedback, will be needed to develop the observed strength.

Brandt et al. (2011) argue for the importance of intrinsic variability in the ocean. The deep equatorial Atlantic features vertically alternating zonal jets that vary at a period of 4.5 years (Lebedev et al. 2007), and display upward energy propagation (Bunge et al. 2008). Brandt et al. (2011) suggest that this variability pattern in the deep ocean, associated with the basin mode, may be able to imprint on the surface circulation and thus promote interannual variability in the 4.5-year range. Thus, there is a suggestion that intrinsic oceanic variability may be able to influence the AZM.

5. Linkage to tropical Atlantic variability

As suggested in section 4.8, the AZM may be closely linked to other modes of tropical Atlantic variability. Here we examine these links in more detail.

5.1. Link to the meridional mode

The Atlantic meridional mode (AMM) is a pattern of variability characterized by subtropical SST anomalies of opposite sign straddling the equator (Fig. 13; Chang et al. 1997; Ruiz-Barradas et al. 2000). It is thought to arise from coupled air-sea interaction in the form of the wind stress-evaporation-SST (WES) feedback (Xie and Philander 1994). In the WES feedback, an initial warm (cold) anomaly in one hemisphere is accompanied by low (high) sea-level pressure (SLP) anomalies. This leads to a cross-equatorial flow whose zonal component, due to the coriolis force, has opposite signs north and south of the equator. Thus the wind anomalies reinforce the trade winds in one hemisphere and weaken them in the other, leading to latent heat flux anomalies that amplify the pre-existing SST anomalies.

Servain et al. (1999) noted a correlation between indices of the AMM, ATL3 thermocline depth and ITCZ latitude in observations. They suggested that anomalous shifts in ITCZ latitude lead to shifts in the entire trade wind system, which induces zonal wind anomalies on the equator. Foltz and McPhaden (2010b) argued that the AMM exerts two competing influences on the AZM. During positive AMM events, characterized by warming in the northern tropical Atlantic (NTA), the immediate impact on the equator is a strengthening of the zonal winds and Kelvin wave induced cooling in the east. North of the equator, however, the AMM is often accompanied by wind stress curl anomalies that induce downwelling Rossby waves, which upon reflection on the western boundary, lead to warming on the equator. This mechanism has also been discussed in the context of non-canonical events (see section 4.6) and the termination of AZM events (Martin-Rey et al. 2019).

Murtugudde et al. (2001) suggested that the link between AMM and AZM described by Servain et al. (1999) is only strong during certain periods, implying that, on average, the link between them is weaker than suggested by Servain et al. (1999). The relation between equatorial trades and ITCZ latitude, however, seems to be very close even for periods suggested to have a weak link by Murtugudde et al. (2001), as suggested by Richter et al. (2014a) and Fig. 12. It should be noted, on the other hand, that these results concern only the link between ITCZ latitude and equatorial surface winds, not the relation between AMM and AZM per se. As discussed in section 4.3, wind anomalies are not a very good predictor of AZM events due to the existence of non-canonical events, which, in turn, may also be related to the wave-reflection mechanism. Due to the delayed wave feedback, the exact temporal evolution of the AMM may be crucial for the way it influences the AZM. An early onset of wind stress curl anomalies may have a significant impact on the developing phase of AZM events and even change their sign, while a later onset may just contribute to the decay of events.

5.2. Link to the Benguela Niño

The Benguela Niño (*Oettli et al., 2020 review it in Chapter 10 of this book*) is a variability pattern characterized by SST anomalies along the southwestern coast of Africa that occurs on interannual timescales (see Chapter 10). While the maximum variability occurs along the coast, SST anomalies extend into the ocean interior (the March and April panels of Figures 7 and 8 convey a good sense of this mode). Variability in the region is due to upwelling anomalies, which, in turn, can be generated by equatorially forced Kelvin waves that are transmitted into coastally trapped waves at the eastern boundary (e.g. Shannon et al. 1986). This suggests an obvious pathway for a link between the AZM and Benguela Niños because Kelvin waves that are generated predominantly in the western and central

equatorial Atlantic should influence, in sequence, both the eastern equatorial Atlantic and the coast of southwest Africa. While the AZM and Benguela Niño SST time series are indeed well correlated (Lübbecke et al. 2010), the Benguela Niño typically *leads* the AZM, leading to an apparent conundrum that has not been fully resolved. More discussion on this can be found in Chapter 10.

The signature of the Benguela Niño is clearly visible in the structure of the AMM (Fig. 13). As the AZM and Benguela Niño tend to be of the same sign during a given year, they form part of the southern pole of the AMM. As discussed in 5.1, zonal wind anomalies typically display a sign change north of the equator. Thus, the trade wind anomalies north of the equator will help to establish SST anomalies that are of opposite sign to those on and south of the equator. This relation, however, is not consistently observed and some studies have questioned the existence of a "dipole mode" (Dommenget and Latif 2000). Thus, while there is a potential mechanism for a dipole, complicating factors may obscure this relation.

6. Relations of equatorial Atlantic variability to terrestrial precipitation and remote basins

While the AZM amplitude is weaker than that of ENSO, it has been shown to influence precipitation over the surrounding continents. More recently, some studies suggest that the AZM can even influence ENSO. Conversely, the influence of ENSO on the northern tropical Atlantic has long been established but its influence on the equatorial Atlantic and the AZM is inconsistent. In the following we take a closer look at these teleconnections.

6.1. Impact on tropical precipitation

Warm AZM events are associated with increased precipitation over the equatorial Atlantic and the Guinea coast just to the north. On interannual timescales, this is the most robust impact on African rainfall of any of the tropical Atlantic SST variability patterns (Rowell et al. 2013). This impact can be seen in our AZM composites (Figs. 7 and 8) and has been well documented in the literature (Hastenrath and Lamb 1977; Hastenrath 1984; Horel et al. 1986; Wagner and da Silva 1994; Okumura and Xie 2004; Rowell 2013; Lutz et al. 2015; see also review by Rodriguez-Fonseca et al. 2015). These rainfall anomalies can be explained by the destabilizing impact of the warm SST anomalies on the overlying atmosphere. Particularly in late spring and early summer, when the West African monsoon develops, the prevailing southerly surface winds can carry warm moist air toward the Guinea coast and fuel increased precipitation there. As the moisture rains out over the coast, less moisture is available downstream for the Sahel region and, consistently, warm AZM events are associated with reduced rainfall (Rowell et al. 1995; Janicot et al. 1998), though the link is somewhat weaker than that with the Guinea coast and is not evident in our composites. The lack of a robust response in Sahel precipitation may be due to the competing influence from the tropical Pacific, which has gained prominence in recent decades (Losada et al. 2012).

The AZM is also associated with rainfall anomalies over northeast South America (Figs. 7 and 8). In the spring of positive AZM events, there is an anomalous southward shift and strengthening of the ITCZ precipitation over South America (Fig. 7), which leads to a north-south dipole in precipitation anomalies. While these anomalies are statistically related to the AZM, it is not clear to what extent they are driven by it. The southward shift of the ITCZ in early spring, for example, occurs during a time when the SST anomalies are

still weak and may thus be seen as a driver of westerly wind events and the AZM. At the same time, the early stages of the AZM are typically associated with an AMM-like pattern that may have a larger impact on ITCZ position than the local SST anomalies associated with the AZM.

Some studies have suggested that the AZM may even influence the Indian summer monsoon (Kucharski et al. 2007; Kucharski et al. 2008; Pottapinjara et al. 2014). According to these studies, a warm AZM event warms the troposphere over the tropical Indian Ocean through the Gill (1980) mechanism. This leads to a stabilization of the atmospheric column, a reduction in the number of monsoon depressions, and less rain over land. Pottapinjara et al. (2014) argue that this mechanism should be particularly important during neutral ENSO years.

6.2. Impact of the AZM on ENSO

A study by Rodriguez-Fonseca et al. (2009) brought attention to the possibility that the AZM may enhance or even trigger ENSO, and that the strength of this influence may be subject to decadal modulation. While, compared to ENSO, the SST anomalies of the AZM are of weak amplitude and small spatial extent, they occur during late spring and early summer, when SST anomalies are still weak in the equatorial Pacific.

The proposed mechanism for the equatorial Atlantic influence on ENSO is through modulation of the Walker circulation (Rodriguez-Fonseca et al. 2009; Losada et al. 2010; Ding et al. 2012; Kucharski et al. 2016). During positive AZM events, convection and upper level divergence are strengthened over the central equatorial Atlantic. This is compensated, in part, by descending motion and easterly surface wind anomalies over the central and western equatorial Pacific. Such wind anomalies trigger upwelling Kelvin waves that drive SST cooling toward the east, enhancing the chance of La Niña development.

Thus, positive AZM events may assist in the development of opposite signed ENSO events. A study by Jia et al. (2019) suggests that this influence may be weakening under global warming due to the stabilization of the troposphere.

Several studies suggest that ENSO prediction can be enhanced when SST anomalies are prescribed in the tropical Atlantic (Frauen and Dommenget 2012; Dayan et al. 2014) or even in the equatorial Atlantic only (Keenlyside et al. 2013), supporting the idea that remote impacts from the Atlantic have the potential to alter ENSO development.

Notwithstanding the supportive evidence above, there remains considerable uncertainty regarding the equatorial Atlantic influence on ENSO. While the AZM tends to peak about half a year before ENSO, both events usually start developing in boreal spring. Thus, it is difficult to establish the directionality of interbasin influences based on observational studies alone. Numerical experiments can be helpful in this regard but are not unambiguous either; restoring SSTs to observations in the tropical Atlantic, e.g., may implicitly introduce information from the Pacific, as the Pacific remotely influences Atlantic SST. In the context of prediction experiments, this may lead to an overestimate of the skill that can be gained from tropical Atlantic variability, as noted by Keenlyside et al. (2013).

6.3. Impact of ENSO on the AZM

Despite ENSO's far reaching impacts around the globe, its impacts on the equatorial Atlantic are surprisingly inconsistent (Chang et al. 2006; Lübbecke and McPhaden 2010), with the instantaneous correlation between ENSO and AZM indices close to zero (e.g. Tokinaga et al. 2019). Perhaps most puzzling is the fact that two of the strongest El Niño events on record (1982 and 1997) were followed by AZM events of opposite sign (negative and positive, respectively). This inconsistent relation can partly be explained by the different seasonality of the two phenomena: ENSO is still in its early development when the

AZM develops and therefore cannot exert its full strength on the equatorial Atlantic. This, however, may only be part of the explanation. Chang et al. (2006) suggest that El Niño has two competing impacts on the equatorial Atlantic: a thermodynamic and a dynamical one. The thermodynamic influence consists of tropospheric warming over the tropical Atlantic, which leads to SST warming. The dynamic influence is a change in the Walker circulation that leads to easterly surface wind anomalies and thus cools the equatorial Atlantic. Chang et al. (2006) argue that, due to these competing effects, the net response of the equatorial Atlantic is often weak.

Lübbecke and McPhaden (2012) point to the opposing surface wind anomalies on and north of the equator that typically occur during ENSO. When positive SST anomalies are present in the tropical Pacific during boreal spring, the Atlantic northeast trade winds weaken and NTA SSTs warm, a well-established and robust impact of ENSO (e.g. Enfield and Mayer 1997). Combined with the strengthening of the equatorial trades this leads to negative wind stress curl anomalies and downwelling just north of the equator. As described in section 4.6, subsequent Rossby wave reflection (Lübbecke and McPhaden 2012) or meridional advection (Richter et al. 2013) can eventually lead to warming on the equator, which opposes the SST anomalies that were generated by local dynamical processes.

Tokinaga et al. (2019) show that, for multi-year ENSO events, there *is* a consistent influence on the equatorial Atlantic. Their results indicate that, during multi-year events, zonal SST gradients across the western and central equatorial Pacific persist well into the spring following the ENSO peak. This, they argue, allows the tropical Pacific to have a strong influence on the equatorial Atlantic, whereas single-year events decay too quickly in spring.

Inconsistency of the Pacific-Atlantic relation may also arise through the modulation of teleconnections by the background state. Based on observational analysis, Martin-Rey et al. (2014) suggest that the Atlantic multi-decadal oscillation (AMO; also referred to as Atlantic Multidecadal Variability or AMV) modulates the link between ENSO and the AZM. According to their study, the interbasin link is strong during negative phases of the AMV, when SSTs are anomalously warm in the southern hemisphere, which is accompanied by a southward shift of the Atlantic ITCZ. There is substantial uncertainty, however, because the observational record is too short to reliably assess multidecadal variability, and model simulations suffer from severe biases. The latter will be the topic of the next section.

7. Representation of equatorial Atlantic variability in GCMs

7.1. Mean state biases

While the observed equatorial Atlantic features a pronounced zonal SST gradient in the annual mean, with warm SST in the west and cool SST in the east, GCMs struggle to reproduce this gradient and, in some cases, even reverse it. An intercomparison study by Davey al. (2002) was perhaps the first to point out the pervasiveness of this problem across models. Subsequent multi-model studies not only confirmed that this bias is near-universal but also showed that it has improved little despite decades of model development (Richter and Xie 2008; Richter et al. 2014a), though a recent study suggests that a few CMIP6 models have relatively small equatorial Atlantic biases (Richter and Tokinaga 2020).

Equatorial SST biases are related to the underrepresentation of the equatorial Atlantic cold tongue, which is most developed in boreal summer. As a consequence, the SST biases also display a clear seasonality, with the weakest biases in spring and the most severe biases in summer (Fig. 14; Chang et al. 2007; Richter and Xie 2008). This is in marked contrast

to the equatorial surface westerly wind bias, which is most pronounced in spring but weak in summer and other seasons (Fig. 14). In addition, AGCMs forced with observed SSTs do still produce a pronounced westerly bias in spring (Richter and Xie 2008; Richter et al. 2014a; Richter and Tokinaga 2020). Based on these facts, Chang et al. (2007) and Richter and Xie (2008) suggest that a significant portion of the equatorial Atlantic SST biases is due to deficiencies in the atmospheric model component, which produces a westerly wind bias even in the absence of SST biases. In coupled ocean-atmosphere models, such a westerly bias deepens the thermocline in the east (approximated by the depth of the 20°C isotherm in Fig. 14), which renders upwelling-related cooling less effective in summer, when the cold tongue is observed to form. As a result, the most severe SST bias is seen in July.

Several subsequent studies have confirmed the important role of equatorial surface wind biases (Wahl et al. 2011; Richter et al. 2012; Zermeño-Diaz and Zhang 2013; Richter et al. 2014a; Voldoire et al. 2019). Errors in the oceanic model components, however, also likely play an important role, as shown by several other studies (Hazeleger and Haarsma 2005; Jochum et al. 2012; Xu et al. 2014a; Song et al. 2015). In particular the representation of the sharp equatorial thermocline and vertical mixing in the upper ocean pose a challenge to models.

In addition to equatorial SST and wind, several other aspects are subject to biases. This includes underrepresentation of stratocumulus clouds and warm SST biases in the southeastern tropical Atlantic (see Richter 2015 and Zuidema et al. 2016 for reviews), an Atlantic ITCZ that is erroneously placed south of the equator in spring, deficient precipitation over northeast South America, and excessive precipitation over Africa (e.g. Richter et al. 2016). The southeast Atlantic SST biases may be related to the equatorial ones through the

equatorial-coastal wave guide (Xu et al. 2014a). In turn, the southeast Atlantic warm bias may contribute to the southward shift of the Atlantic ITCZ (Xu et al. 2014b), though there might be some model dependence regarding this impact (Small et al. 2015).

7.2. Errors in the simulated variability

In spite of their severe mean state errors, many models produce a mode of variability that has similarities with the observed AZM in terms of spatial structure and temporal evolution, including phase locking to summer (Richter et al. 2014a; Richter and Tokinaga 2020). The simulated AZM, however, is typically too weak and peaks one month later than observed (Fig. 15; Richter et al. 2014a). This is consistent with a generally slower cold tongue formation and equatorial trade wind strengthening (Fig. 16). The origin of this delay in the seasonal cycle is unclear but it may be related to the unrealistic southward excursion of the ITCZ in spring, which has a strong impact on surface winds and, subsequently, SST. The southward excursion and delayed northward migration of the ITCZ are associated with the late onset of the West Africa monsoon in simulations (Steinig et al. 2018).

The relation between ITCZ latitude and strength of the equatorial surface zonal wind stress is reproduced by GCMs in a general sense (Fig. 12), though there is one qualitative difference: the simulated ITCZ can shift farther south than the observed one. This has important implications for the mean state biases. Due to the close association of ITCZ latitude and equatorial surface wind stress the southward position of the ITCZ translates into weak equatorial trades in simulations. This hints that misrepresentation of deep convection lies at the heart of the equatorial Atlantic bias problem.

Several studies suggest that the excessively deep thermocline in many models renders upwelling related cooling less effective (Deppenmeier et al. 2016; Dippe and Greatbatch 2017; Jouanno et al. 2017). This weakens the Bjerknes feedback and thus reduces the role

of ocean dynamics. Instead, thermodynamic processes, especially surface latent heat flux, may exert a stronger control on SST variability in such models (Ding et al. 2015; Dippe and Greatbatch 2017; Jouanno et al. 2017). In addition to an excessively deep mean thermocline, errors in the seasonal cycle of both SST and thermocline may also affect the simulated interannual variability (Ding et al. 2015; Prodhomme et al. 2019)

The spatial structure of the AZM is captured relatively well by several GCMs (Richter et al. 2014a), with SST warming in the central and eastern equatorial Atlantic and along the southwest African coast. In some of the models, the amplitude of both SST and surface wind anomalies is greater than observed, and in most of them the SST signature is too narrowly confined along the equatorial-coastal wave guide. This gives the impression that upwelling plays too prominent a role in the development of the SST anomalies but could also mean that other processes that spread the SST anomalies horizontally are poorly represented. The former would be in contradiction to the above-mentioned studies that suggest underestimation of dynamical processes in GCMs.

8. Prediction of equatorial Atlantic variability

Prediction of equatorial Atlantic interannual variability is a longstanding challenge for GCM prediction systems (Stockdale et al. 2006; Richter et al. 2018), with the skill of dynamical forecasts often matched or even outperformed by persistence forecasts and simple statistical models. This is in stark contrast to the equatorial Pacific, where dynamical forecasts clearly outperform persistence. There are two possible explanations for the Atlantic predictability hurdle: 1) Current prediction models are inadequate. This could be due to systematic errors in the model formulation, insufficient observations to initialize the mod-

els, or shortcomings in the initialization procedure (data assimilation etc.). 2) The theoretical predictability of the equatorial Atlantic is inherently low, due to, e.g., weak coupled feedbacks or internal variability.

The relative roles of 1) and 2) in the predictability hurdle is difficult to estimate. The few studies that have systematically investigated the link between systematic model errors and prediction skill typically obtained ambiguous results (see Richter et al. 2018 for a discussion), though they do point to a link. Two recent studies suggest that there is a strong link between skill and variability errors, if the latter are severe (Dippe and Greatbatch 2019; Noel Keenlyside, personal communication). While alleviating biases in these models through flux correction showed significant skill improvement, the flux-corrected models could only rise to about the skill of the persistence forecast. Thus it remains an open question, whether the current low skill in hindcast experiments (Richter et al. 2018) can be significantly enhanced by fixing model errors.

Several studies suggest that the Bjerknes feedback in the equatorial Atlantic is much weaker than in the Pacific (Zebiak 1993; Keenlyside and Latif 2007; Richter et al. 2014b; Deppenmeier et al. 2016; Lübbecke and McPhaden 2013). Richter et al. (2017) point out that coupled feedbacks are only strong during a relatively short period (approximately April and May), leaving little time for AZM growth through dynamical processes. The results of Nnamchi et al. (2015, 2016), by pointing to a significant role of thermodynamic processes, also imply a weaker role of dynamic processes. Regarding the influence of SST biases on model performance, Richter et al. (2018) showed that when an AGCM is forced with observed SST anomalies added to a severely biased SST climatology, surface wind anomalies are quite realistic. This suggests that AGCMs can produce a realistic response

to SST anomalies even in the presence of mean state biases and, by extension, that SST biases are not a major reason for the poor prediction skill (though oceanic subsurface temperature biases might be). This could mean that only moderate gains in prediction skill can be expected from fixing model errors. Additionally, the relatively strong role of atmospheric internal variability in the equatorial Atlantic (Richter and Doi 2019) suggests that inherent predictability may be relatively low in the equatorial Atlantic. On the other hand, we do not know exactly how close to the limit current prediction systems are. Thus, there is the possibility that skill improvement can be obtained through a denser observational network (Tompkins and Feudale 2010) or refined initialization procedures. In any event, more work will be needed to quantify the limits of equatorial Atlantic predictability and the role of model errors.

9. Low-frequency modulation of equatorial Atlantic variability and the impact of climate change

The observational record of Atlantic SST roughly extends from the 1870s to present, but spatial coverage is mostly limited to commercial shipping routes until the advent of the satellite observation era in the late 1970s. Estimating decadal and longer variability from these data poses a challenge, as is projecting future changes based on biased GCMs. We therefore keep brief the discussion of these aspects.

Decadal-to-interdecadal variability in the Atlantic basin is dominated by the AMV. During the negative phase of the AMV, SSTs are warmer than normal on and south of the equator (Kerr 2000; Knight et al. 2006), which is associated with a southward shift of the ITCZ and weakening of the equatorial trades. This should lead to deepening of the thermocline and reduce SST variability in the eastern equatorial Atlantic (Haarsma et al. 2008;

Polo et al. 2013). Martin-Rey et al. (2018), on the other hand, find a shoaling of the thermocline that is associated with a higher amplitude of the AZM. This is partially supported by Svendsen et al. (2014), who find a strengthening of the equatorial Atlantic zonal SST gradient during negative AMV events.

Strengthening and further westward extent of AZM events may also alter the teleconnections of the AZM, since convection is most active in the central and western part of the basin. In combination with the warming of the equatorial background state, this leads to stronger remote influences, particularly on the equatorial Pacific (Svendsen et al. 2014; Losada and Rodriguez-Fonseca 2016).

There is evidence that the equatorial cold tongue and trades have weakened and that the thermocline has deepened during the period 1950-2009 (Tokinaga and Xie 2011). According to the authors, this is associated with reduced SST variability in the eastern equatorial Atlantic. These results partially conflict with those of Martin-Rey et al. (2018), who suggest strengthening of AZM variability during the recent negative phase of the AMV. The weakening of the trades also needs to be reconciled with the observations of Servain et al. (2014), who find trade wind strengthening over the entire tropical Atlantic. The ATL3 time series (Fig. 6) is suggestive of a reduction in variability during the last seven decades, consistent with the result of Tokinaga and Xie (2011). Much more analysis will be needed, however, to assess the relative roles of decadal modulation, greenhouse gas forcing, and intrinsic variability (for the last, see Wittenberg et al. 2009 who discuss this problem in the context of ENSO).

While the tropical Atlantic and most of the other tropical areas have warmed in recent decades, the eastern tropical Pacific has been subject to cooling (Kosaka and Xie 2013),

with implications on global climate. Li et al. (2016) argue that the tropical Atlantic warming has played an important role in this by inducing easterly anomalies over the equatorial Pacific that strengthened upwelling-related cooling in the region. Historical simulations in the CMIP5 archive are unable to replicate cooling periods of similar length in the eastern tropical Pacific. McGregor et al. (2018) attribute this underestimation of decadal variability to the remote impacts of tropical Atlantic SST biases.

The above discussion indicates that much work remains to verify historical trends and to build confidence in global warming projections for the tropical Atlantic region and beyond.

10. Summary and open questions

In this chapter, we have reviewed variability in the equatorial Atlantic with a focus on the Atlantic zonal mode (AZM), a pattern of interannual variability that resembles ENSO in the Pacific.

10.1. Summary

The AZM is characterized by SST warming in the eastern and central equatorial Atlantic that typically starts in early boreal spring, peaks in early summer, and decays in late summer and early fall. SST variability has an amplitude of 1 K and shows spectral peaks at periods of about 1.5-4.5 years, though these are not distinct from red noise. SST warming is often preceded by westerly wind events over the western equatorial Atlantic, suggesting a dynamic generation mechanism similar to ENSO, in which downwelling Kelvin waves deepen the eastern thermocline and weaken cold tongue formation in the following months. There are, however, also warm events that are preceded by easterly wind anomalies. During

these events, off-equatorial processes, such as oceanic Rossby waves and meridional temperature advection, seem to play an important role.

Coupled feedbacks, in particular the Bjerknes feedback, appear to be active but are mostly limited to April and May. Before April, SST anomalies tend to be too weak to initiate coupling, while after May the ITCZ migrates away from the equator (regardless of any existing SST anomalies), which drastically weakens coupling strength. Together with the significant influence of thermodynamics processes, and the relatively large role of internal atmospheric variability, this suggests relatively low predictability of the AZM, which is consistent with current prediction systems struggling to beat persistence.

The AZM appears to be linked to the Atlantic meridional mode (AMM), a pattern of opposite-signed SST anomalies north and south of equator. This link can be explained through the wider circulation changes that accompany AZM events. In the early phase of positive AZM events, the ITCZ shifts southward and trade winds strengthen north of the equator but weaken on the equator and to the south of it. The resultant latent heat flux anomalies lead to SST cooling to the north and warming to the south, which may be further amplified through the WES feedback. The Benguela Niño in the southeastern tropical Atlantic, which is located within the southern lobe of the AMM, is also closely linked to the AZM. This link can be explained through Kelvin waves along the equatorial-coastal waveguide, but also, to some extent, through the basin-wide wind anomalies.

ENSO has a strong and robust influence on the northern tropical Atlantic but the influence of ENSO on the AZM is weak and inconsistent. Explanations for this include the competition of dynamical and thermodynamical influences, the northequatorial wind stress

curl anomalies that often accompany ENSO events, and the sensitivity to the timing of ENSO decay.

The AZM itself may be able to contribute to the development of ENSO events, and may also have an influence on the Indian summer monsoon. It appears though, that these relations are subject to decadal-scale modulation.

Finally, the AZM and its remote influences may be weakening under the influence of greenhouse gas forcing, but much work remains to be done to confirm this.

10.2. Open questions

While much progress has been achieved in understanding the equatorial Atlantic mean state and variability, many interesting questions and puzzles remain. Here we list some questions we regard as central. We stress that this selection is very subjective.

10.2.1 What maintains the equatorial surface easterlies in boreal spring?

The pressure gradient force by itself would mandate westerlies over much of the basin width but easterlies are observed. It has been hypothesized that vertical momentum transport plays a crucial role but, to the authors' knowledge, no study has systematically analyzed this. (cf. section 3.1)

10.2.2 What is the role of atmospheric vertical momentum transport in interannual variability?

Previous studies have hinted that vertical momentum transport also plays a crucial role in interannual variability, and that the decay of events is triggered by the decrease of vertical momentum transport that occurs when the ITCZ migrates away from the equator. Much

more work remains to be done to understand the role of vertical momentum transport. (cf. section 4.3)

10.2.3 What is the cause of the asymmetric relation between equatorial surface zonal winds and Atlantic ITCZ latitude?

There is a close relation between ITCZ latitude and the strength of the equatorial easterlies in the western part of the basin. This relation is not symmetric about the equator because winds are strong when the ITCZ is north of the equator but weak when it is on or south of the equator. The cause of this asymmetry remains unknown. It may be related to the geometries of South America and Africa or to the nature of the convective systems that constitute the ITCZ. (cf. section 4.8)

10.2.4 What causes the inconsistent influence of ENSO on the AZM?

Several hypotheses have been put forward but their relative merits await further exploration. None of them can satisfactorily explain the opposite outcomes of the 1982 and 1997 El Niños. (cf. section 6.3)

10.2.5 To what extent does equatorial Atlantic variability contribute to the development of ENSO events?

It is clear that the equatorial Atlantic must have some influence on ENSO but, given the small amplitude and geographical extent of the AZM, the question is how important this influence can be. Observations may not be sufficient to solve this problem because the

record is relatively short and because both events tend to develop in boreal spring. (cf. section 6.2)

10.2.6 What are the theoretical limits of AZM predictability?

Recent studies suggest that predictability of the AZM is inherently low but much more work has to be done to quantify this. (cf. section 8)

10.2.7 What is the role of GCM mean state biases in the tropical Atlantic on basin interaction and global warming projections?

GCM biases in the tropical Atlantic have proven to be hard to fix and may continue to pose a challenge in the foreseeable future. Thus, it is important to understand how these biases influence other basins, and how they might affect global warming projections. While a few studies have started to address this, much work remains to be done. (cf. section 9).

10.3. Ways forward

Finally, we comment on how the questions raised in 10.2 may be addressed.

Convective momentum transport (10.2.1 and 10.2.2) is difficult to observe as it requires precise measurements of horizontal and vertical velocity at high temporal resolution in adverse weather conditions. Nevertheless, there are measurements that can be leveraged, including field campaigns that are ongoing (Bony et al. 2017) or being planned (Bjorn Stevens, personal communication). Explicitly simulating convective momentum transport requires models with very high resolution (~ a few kilometers horizontally) in the tropical Atlantic. Such simulations are becoming increasingly feasible, and it will be exciting to see what can be learned from them. Both the aforementioned observations and simulations may also shed light on the asymmetric relation between ITCZ latitude and equatorial surface

winds (10.2.3). In addition, GCM sensitivity experiments with idealized changes in the continental geometry may help to solve this puzzle.

GCM experimentation may also help in disentangling the two-way interaction between the tropical Pacific and tropical Atlantic (10.2.5 and 10.2.6). Coordinated multi-model experiments could be a valuable tool for this, and the authors are part of an effort to set up such a model intercomparison. In addition, long-term climate records, such as those obtained from coral proxies, could provide a means to corroborate results obtained from the observational record (e.g. Tierney et al. 2015).

Quantifying the limits of AZM predictability (10.2.6) is a tough problem and any results may eventually be rendered obsolete by the actual skill improvements of prediction systems. To wit, a recent multi-model skill assessment suggests substantial improvements in the equatorial Atlantic (Chloe Prodhomme, personal communication). Nevertheless, attempting to quantify skill limits should remain an important endeavor that can guide improvement efforts. This will require quantifying the stochastic component of the system, as well as clarifying the impact of model biases on prediction skill. Neither of these two topics has received much attention so far. Exploring the limits of predictability will also require assessing the benefit of observational networks (e.g. data denial experiments) and initialization procedures (e.g. coupled data assimilation).

The impact of mean state biases on inter-basin interaction and global warming projections (10.2.7) is another difficult problem. Numerical experiments with prescribed SST can partially address this issue but suffer from all the potential inconsistencies of fixing one component of a coupled system. A recent intercomparison of CMIP6 models suggests that a few models now have relatively small biases in the tropical Atlantic, while at the same

time producing relatively realistic interannual variability (Richter and Tokinaga 2020). Thus, there is now a wide range of model behavior (from light to severe model errors) that may allow systematic study of the impacts of tropical Atlantic biases on basin interaction and climate change projections.

Acknowledgments

The authors thank Prof. Noel Keenlyside for his insightful comments on the manuscript. The authors were partially supported by the Japan Society for the Promotion of Science, KAKENHI Grant 18H01281.

References

Adamec, D., and J. J. O'Brien, 1978: The seasonal upwelling in the Gulf of Guinea due to remote forcing. *J. Phys. Oceanogr.,* **8,** 1050–1060.

Adler, R. F., and Coauthors, 2018: The Global Precipitation Climatology Project (GPCP) monthly analysis (new version 2.3) and a review of 2017 global precipitation. *Atmosphere*, **9**, 138, https://doi.org/10.3390

Balmaseda, M. A., Mogensen, K. and Weaver, A. T. (2013), Evaluation of the ECMWF ocean reanalysis system ORAS4. Q.J.R. Meteorol. Soc., 139: 1132–1161. doi: 10.1002/qj.2063

Battisti, D. S., and Hirst, A. C. (1989), Interannual variability in the tropical atmosphere ocean model: Influence of the basic state, ocean geometry and nonlineary, J. Atmos. Sci., 45, 1687– 1712.

Bony, S., and Coauthors, 2017: EUREC4A: A field campaign to elucidate the couplings between clouds, convection and circulation. *Surv. Geophys.*, **36**, 73–40, https://doi.org/10.1007/s10712-017-9428-0.

Bourlès, B., Araujo, M., McPhaden, M. J., Brandt, P., Foltz, G. R., Lumpkin, R., Giordani, H., Hernandez, F., Lefevre, N., Nobre, P., Campos, E., Saravanan, R., Trotte-Duha, J., Dengler, M., Hahn, J., Hummels, R., Lubbecke, J. F., Rouault, M., Cotrim, L., Sutton, A., Jochum, M., & Perez, R. C. (2019). PIRATA: A sustained observing system for tropical Atlantic climate research and forecasting. Earth and Space Science, 6, 577– 616.

Brandt, P., Funk, A., Hormann, V., Dengler, M., Greatbatch, R. J., & Toole, J. M. (2011). Interannual atmospheric variability forced by the deep equatorial Atlantic Ocean. Nature, 473, 497–500. https://doi.org/10.1038/nature10013

Bunge, L., Provost, C., Hua, B. L. & Kartavtseff, A., 2008: Variability at intermediate depths at the equator in the Atlantic Ocean in 2000–06: annual cycle, equatorial deep jets, and intraseasonal meridional velocity fluctuations. J. Phys. Oceanogr. 38, 1794–1806.

Burmeister, K., Brandt, P., & Lübbecke, J. F. (2016). Revisiting the cause of the eastern equatorial Atlantic cold event in 2009. Journal of Geophysical Research: Oceans, 121, 4777– 4789. https://doi.org/10.1002/2016JC011719

Busalacchi, A. J., and J. Picaut, 1983: Seasonal variability from a model of the tropical Atlantic Ocean. *J. Phys. Oceanogr.,* **13,** 1564–1588.

Chang CY, Carton JA, Grodsky SA, Nigam S (2007) Seasonal climate of the tropical Atlantic sector in the NCAR community climate system model 3: error structure and probable causes of errors. J Clim 20:1053–1070

Chang, P., L. Ji, and H. Li, 1997: A decadal climate variation in the tropical Atlantic Ocean from thermodynamic air-sea interactions. *Nature*, **385,** 516–518.

Chang, P., Y. Fang, R. Saravanan, L. Ji, and H. Seidel, 2006: The cause of the fragile relationship between the Pacific El Niño and the Atlantic Niño. *Nature*, **443,** 324–328.

Clement, A., P. DiNezio, and C. Deser, 2011: Rethinking the ocean's role in the Southern Oscillation. *J. Climate*, **24**, 4056–4072.

Dayan, H., Vialard, J., Izumo, T., & Lengaigne, M. (2014). Does sea surface temperature outside the tropical Pacific contribute to enhanced ENSO predictability? Climate Dynamics, 43(5–6), 1311–1325.

Davey MK et al (2002) STOIC: a study of coupled model climatology and variability in topical ocean regions. Clim Dyn 18:403–420

Deppenmeier, A. L., Haarsma, R. J., & Hazeleger, W. (2016). The Bjerknes feedback in the tropical Atlantic in CMIP5 models. Climate Dynamics, 47, 2691–2707. https://doi.org/10.1007/s00382-016-2992-z

Ding, H., N. S. Keenlyside, and M. Latif, 2010: Equatorial Atlantic interannual variability: the role of heat content, JGR Oce., 115, C09020

Ding, H., Keenlyside, N. S., & Latif, M. (2012). Impact of the equatorial Atlantic on the El Niño Southern Oscillation. Climate Dynamics, 38, 1965–1972. https://doi.org/10.1007/s00382-011-1097-y

Dippe, T., Greatbatch, R. J., & Ding, H. (2017). On the relationship between Atlantic Niño variability and ocean dynamics. Climate Dynamics. https://doi.org/10.1007/s00382-017-3943-z

Dippe, T., R. J. Greatbatch, H. Ding, 2019: Seasonal prediction of equatorial Atlantic sea surface temperature using simple initialization and bias correction techniques. Atmos. Sci. Lett.; https://doi.org/10.1002/asl.898

Dommenget, D., and M. Latif, 2000: Interannual to decadal variability in the tropical Atlantic. *J. Climate*, **13,** 777–792.

Eisenman, I., L. Yu, and E. Tziperman, 2005: Westerly wind bursts: ENSO's tail rather than the dog? *J. Climate*, **18,** 5224–5237.

Enfield, D. B., and D. A. Mayer, 1997: Tropical Atlantic sea surface temperature variability and its relation to El Niño–Southern Oscillation. J. Geophys. Res., 102, 929–946.

Foltz, G. R., Grodsky, S. A., Carton, J. A., and McPhaden, M. J. (2003). Seasonal mixed layer heat budget of the tropical Atlantic Ocean. J. Geophys. Res.-Oceans 108:3146. doi: 10.1029/2002JC001584

Foltz, G. R., and McPhaden, M. J. (2010a). Abrupt equatorial wave-induced cooling of the Atlantic cold tongue in 2009. Geophys. Res. Lett. 37:L24605. doi: 10.1029/ 2010GL045522

Foltz, G. R., and McPhaden, M. J. (2010b). Interaction between the Atlantic meridional and Nino modes. Geophys. Res. Lett. 37:L18604. doi: 10.1029/ 2010GL044001

Foltz, G. R., and Coauthors, 2019: The tropical Atlantic observing system, Front. Mar. Sci., https://doi.org/10.3389/fmars.2019.00206

Frauen, C., & Dommenget, D. (2012). Influences of the tropical Indian and Atlantic Oceans on the predictability of ENSO. Geophysical Research Letters, 39(2).

Frierson DMW, Hwang Y-T (2012) Extratropical influence on ITCZ shifts in slab ocean simulations of global warming. J Clim 25:720-733

Giannini, A., J. C. H. Chiang, M. A. Cane, Y. Kushnir, and R. Seager, 2001: The ENSO teleconnection to the tropical Atlantic Ocean: Contributions of the remote and local SSTs to rainfall variability in the tropical Americas. *J. Climate*, **14**, 4530–4544.

Gill, A. (1980). Some simple solutions for heat-induced tropical circulation. Quarterly Journal of the Royal Meteorological Society, 106(449), 447–462.

Haarsma, R. J., E. Campos, W. Hazeleger, and C. Severijns, 2008: Influence of the meridional overturning circulation on tropical Atlantic climate and variability. J. Climate, 21, 1403–1416, https://doi.org/10.1175/2007JCLI1930.1.

Harrison, D. E., and G. A. Vecchi, 1997: Westerly wind events in the tropical Pacific, 1986–95. *J. Climate*, **10,** 3131–3156.

Hastenrath, S., 1984: Interannual variability and annual cycle: Mechanisms of circulation and climate in the tropical At- lantic sector. Mon. Wea. Rev., 112, 1097–1107, doi:10.1175/ 1520-0493(1984)112,1097:IVAACM.2.0.CO;2.
Hastenrath, S., and L. Heller, Dynamics of climate hazards in Northeast Brazil, Q. J. R. Meteorol. Soc., 103, 77-92, 1977.
Hastenrath, S., and P. J. Lamb, 1977: Some aspects of circulation and climate over the eastern equatorial Atlantic. Mon. Wea. Rev., 105, 1019–1023, doi:10.1175/1520-0493(1977)105,1019: SAOCAC.2.0.CO;2.
Hazeleger, W., & Haarsma, R. J. (2005). Sensitivity of tropical Atlantic climate to mixing in a coupled ocean–atmosphere model. Climate Dynamics, 25, 387–399.
Hersbach, H., and Coauthors, 2018: Operational global reanalysis: progress, future directions and synergies with NWP, ECMWF ERA Report Series 27.
Hisard, P. (1980). Observation de réponses de type “El Niño” dans l'Atlantique tropical oriental Golfe de Guinée. Oceanologica Acta, 3, 69–78.
Horel, J. D., V. E. Kousky, and M. T. Kagano, 1986: Atmospheric conditions in the Atlantic sector during 1983 and 1984. Nature, 322, 248–251, doi:10.1038/322248a0.
Janicot, S., A. Harzallah, B. Fontaine, and V. Moron (1998), West African monsoon dynamics and eastern equatorial Atlantic and Pacific SST anomalies (1970–1988), J. Clim., 11, 1874–1882, doi:10.1175/1520- 0442-11.8.1874.
Jia, F., W. Cai, L. Wu, B. Gan, G. Wang, F. Kucharski, P. Chang, and N. Keenlyside (2019), Weakening Atlantic Niño–Pacific connection under greenhouse warming, Science Advances, 5(8), eaax4111, 10.1126/sciadv.aax4111.
Jin, F. F. (1997), An equatorial ocean recharge paradigm for ENSO. Part I: Conceptual model, *J. Atmos. Sci.*, 54, 811– 829.
Jochum, M., B. P. Briegleb, G. Danabasoglu, W. G. Large, N. J. Norton, S. R. Jayne, M. H. Alford, and F. O. Bryan, 2013: The impact of oceanic near-inertial waves on climate. J. Climate, 26, 2833–2844, doi:https://doi.org/10.1175/JCLI-D-12-00181.1.
Jouanno, J., Hernandez, O. and Sanchez-Gomez, E. (2017) Equatorial Atlantic interannual variability and its relation to dynamic and thermodynamic processes, 8 (4), pp. 1061-1069, doi:10.5194/esd-8-1061-2017
Kalnay, E. and Coauthors, 1996: The NCEP/NCAR Reanalysis 40-year Project. Bull. Amer. Meteor. Soc., 77, 437-471.
Kang, S. M., I. M. Held, D. M. W. Frierson, and M. Zhao, 2008: The response of the ITCZ to extratropical thermal forcing: Idealized slab-ocean experiments with a GCM. *J. Climate*, **21**, 3521–3532, https://doi.org/10.1175/2007JCLI2146.1.
Katz, E. J., et al., Zonal pressure gradient along the equatorial Atlantic, J. Mar. Res., 35, 293-307, 1977.
Keenlyside, N. S., and Latif, M. (2007). Understanding equatorial Atlantic interannual variability. *J. Clim.* 20, 131–142. doi: 10.1175/JCLI3992.1
Keenlyside, N. S., Ding, H., & Latif, M. (2013). Potential of equatorial Atlantic variability to enhance El Niño prediction. Geophysical Research Letters, 40(10), 2278–2283.
Kerr, R. A., 2000: A North Atlantic climate pacemaker for the centuries. Science, 288, 1984–1985, https://doi.org/10.1126/ science.288.5473.1984.
Knight, J. R., C. K. Folland, and A. A. Scaife, 2006: Climate im- pacts of the Atlantic multidecadal oscillation. Geophys. Res. Lett., 33, L17706, https://doi.org/10.1029/2006GL026242.

Kosaka, Y., and S.-P. Xie, 2013: Recent global-warming hiatus tied to equatorial Pacific surface cooling. Nature, 501(7467), 403– 407.

Kucharski F, Bracco A, Yoo JH, Moltini F (2007) Low-frequency variability of the Indian monsoon ENSO relationship and the tropical Atlantic: the weakening of the 1980s and 1990s. J Clim 20:4255–4266. doi: 10.1175/JCLI4254.1 CrossRefGoogle Scholar

Kucharski F, Bracco A, Yoo JH, Molteni F (2008) Atlantic forced component of the Indian monsoon interannual variability. Geophys Res Lett 35:1–5. doi: 10.1029/2007GL033037

Kucharski, F., Parvin, A., Rodriguez-Fonseca, B., Farneti, R., Martin-Rey, M., Polo, I., Mohino, E., Losada, T., Mechoso, C.R., 2016: The Teleconnection of the Tropical Atlantic to Indo-Pacific Sea Surface Temperatures on Inter-Annual to Centennial Time Scales: A Review of Recent Findings. Atmosphere, 7, 29.

Latif, M., and A. Grötzner, 2000: The equatorial Atlantic oscillation and its response to ENSO. *Climate Dyn.*, **16,** 213–218.

Lebedev, K. V., Yoshinari, H., Maximenko, N. A. & Hacker, P. W. YoMaHa'07: Velocity Data Assessed from Trajectories of Argo Floats at Parking Level and at the Sea Surface. IPRC Technical Note 4 (International Pacific Research Center, 2007)

Li, X., S.-P. Xie, S. T. Gille, and C. Yoo, 2016: Atlantic-induced pan-tropical climate change over the past three decades. *Nat. Climate Change*, **6**, 275–279, doi:https://doi.org/10.1038/nclimate2840.

Losada, T., B. Rodríguez-Fonseca, S. Janicot, S. Gervois, F. Chauvin, and P. Ruti, 2010: A multi-model approach to the Atlantic equatorial mode: Impact on the West African monsoon. *Climate Dyn.*, **35**, 29–43, doi:https://doi.org/10.1007/s00382-009-0625-5.

Losada, T., Rodriguez-Fonseca, B., Mohino, E., Bader, J., Janicot, S., and Mechoso, C. R. (2012), Tropical SST and Sahel rainfall: A non-stationary relationship, Geophys. Res. Lett., 39, L12705, doi:10.1029/2012GL052423.

Losada, T., & Rodríguez-Fonseca, B. (2016). Tropical atmospheric response to decadal changes in the Atlantic equatorial mode. Climate Dynamics, 47(3–4), 1211–1224.

Lübbecke, J. F., C. W. Boning, N. S. Keenlyside, and S.-P. Xie, 2010: On the connection between Benguela and equatorial Atlantic Niños and the role of the South Atlantic anticyclone. J. Geophys. Res., 115, C09015.

Lübbecke, J. F., and M. J. McPhaden, 2012: On the inconsistent relationship between Pacific and Atlantic Niños. *J. Climate*, **25**, 4294–4303.

Lübbecke, J. F., 2013: Tropical Atlantic warm events. Nat. Geoscience, 6, 22-23.

Lübbecke, J. F. and M. J. McPhaden, 2013: A comparative stability analysis of Atlantic and Pacific Niño modes. J. Climate, 26 (16), pp. 5965-5980, doi: 10.1175/JCLI-D-12-00758.1

Lübbecke, J. F. and M. J. McPhaden, 2017: Symmetry of the Atlantic Niño mode Geophys. Res. Lett., 44, doi: 10.1002/2016GL071829

Lübbecke, J. F., B. Rodríguez-Fonseca, I. Richter, M. Martín-Rey, T. Losada, I. Polo, and N. Keenlyside, 2018: Equatorial Atlantic variability—Modes, mechanisms, and global teleconnections. Wiley Interdiscip. Rev.: Climate Change, 9, e527, https://doi.org/10.1002/wcc.527.

Lutz, K., Jacobeit, J., & Rathmann, J. (2015). Atlantic warm and cold water events and impact on African west coast precipitation. International Journal of Climatology, 35(1), 128–141.

Martin-Rey, M., B. Rodriguez-Fonseca, I. Polo, and F. Kucharski, 2014: On the Atlantic-Pacific Ninos connection: a multidecadal modulated mode. *Clim. Dyn.*, **43**, 3163-3178.

Martin-Rey, M., I. Polo, B. Rodriguez-Fonseca, T. Losada, and A. Lazar, 2018: Is there evidence of changes in tropical Atlantic variability modes under AMO phases in the observational record? J. Clim., 31, 515-536.

Martin-Rey, M., and A. Lazar, 2019: Is the boreal spring tropical Atlantic variability a precursor of the equatorial mode? Clim. Dyn., 53, 2339–2353. https://doi.org/10.1007/s00382-019-04851-9

McCreary, J., J. Picaut, and D. Moore, 1984: Effects of the remote annual forcing in the eastern tropical Atlantic Ocean. *J. Mar. Res.,* **42,** 45–81.

McGregor, S., M. F. Stuecker, J. B. Kajtar, M. H. England, and M. Collins, 2018: Model tropical Atlantic biases underpin diminished Pacific decadal variability. *Nat. Climate Change*, **8**, 493–498, https://doi.org/10.1038/s41558-018-0163-4.

Merle, J., Annual and interannual variability of temperature in the eastern equatorial Atlantic Ocean – hypothesis of an Atlantic El Nino, Oceanol. Acta, 3, 209-220, 1980.

Moore, D., P. Hisard, J. P. McCreary, J. Merlo, J. J. O'Brien, J. Picaut, J. M. Verstraete, and C. Wunsch, 1978: Equatorial adjustment in the eastern Atlantic. *Geophys. Res. Lett.,* **5,** 637–640.

Murtugudde, R. G., J. Ballabrera-Poy, J. Beauchamp, and A. J. Busalacchi, 2001: Relationship between zonal and meridional modes in the tropical Atlantic. *Geophys. Res. Lett.*, **28,** 4463–4466.

Nnamchi, H. C., Li, J., Kucharski, F., Kang, I.-S., Keenlyside, N. S., Chang, P., et al. (2015). Thermodynamic controls of the Atlantic Niño. Nat. Commun. 6:8895. doi: 10.1038/ncomms9895

Nnamchi, H. C., Li, J., Kucharski, F., Kang, I., Keenlyside, N. S., Chang, P., et al. (2016). An equatorial–extratropical dipole structure of the Atlantic Niño. J. Clim. 29, 7295–7311. doi: 10.1175/JCLI-D-15-0894.1

Neelin, J. D., D. S. Battisti, A. C. Hirst, F-F. Jin, Y. Wakata, T. Yamagata, and S. E. Zebiak, 1998: ENSO theory. *J. Geophys. Res.*, **103,** 14261–14290.

Oettli, P., C. Yuan, I. Richter, 2020: The Other Coastal Niño/Niña — The Benguela, California and Dakar Niños/Niñas, Tropical and Extratropical Air-Sea Interactions, Ed. S. K. Behera, Elsevier, (in press).

Okumura, Y., and S.-P. Xie, 2004: Interaction of the Atlantic equatorial cold tongue and the African monsoon. *J. Climate*, **17**, 3589–3602.

Okumura, Y., and S.-P. Xie. (2006) Some Overlooked Features of Tropical Atlantic Climate Leading to a New Niño-Like Phenomenon. Journal of Climate 19:22, 5859-5874.

Philander, S. G. H., D. Gu, D. Halpern, G. Lambert, N-C. Lau, T. Li, and R. C. Pacanowski, 1996: Why the ITCZ is mostly north of the equator. J. Climate, 9, 2958–2972.

Planton, Y., A. Voldoire, H. Giordani, G. Caniaux, 2018: Main processes of the Atlantic cold tongue interannual variability. Clim. Dyn., 50, 1495–1512; doi:10.1007/s00382-017-3701-2

Polo, I., B. W. Dong, and R. T. Sutton, 2013: Changes in tropical Atlantic interannual variability from a substantial weakening of the meridional overturning circulation. Climate Dyn., 41, 2765–2784, https://doi.org/10.1007/s00382-013-1716-x.

Pottapinjara V, Girishkumar MS, Ravichandran M, Murtugudde R (2014) Influence of the Atlantic zonal mode on monsoon depressions in the Bay of Bengal during boreal summer. J Geophys Res Atmos. 119:6456–6469. doi: 10.1002/2014JD021494

Pottapinjara, V., M. S. Girishkumar, S. Sivareddy, M. Ravichandran, and R. Murtugudde, 2016: Relation between the upper ocean heat content in the equatorial Atlantic during boreal spring and the Indian monsoon rainfall during June–September. *Int. J. Climatol.*, **36**, 2469–2480.

Prodhomme, C., A. Voldoire, E. Exarchou, A. L. Deppenmeier, J. García-Serrano, and V. Guemas (2019), How Does the Seasonal Cycle Control Equatorial Atlantic Interannual Variability?, Geophys Res Lett, 46(2), 916-922, doi:10.1029/2018GL080837.

Richter, I., and Xie, S.-P. (2008). On the origin of equatorial Atlantic biases in coupled general circulation models. Clim. Dynam. 31, 587–598. doi: 10.1007/ s00382- 008-0364- z

Richter, I., Behera, S. K., Masumoto, Y., Taguchi, B., Komori, N., and Yamagata, T. (2010). On the triggering of Benguela Niños: remote equatorial versus local influences. Geophys. Res. Lett. 37:L20604. doi: 10.1029/2010GL044461

Richter, I., Xie, S.-P., Wittenberg, A. T., and Masumoto, Y. (2012). Tropical Atlantic biases and their relation to surface wind stress and terrestrial precipitation. Clim. Dynam. 38, 985–1001. doi: 10.1007/s00382-011-1038-9

Richter, I., Behera, S. K., Masumoto, Y., Taguchi, B., Sasaki, H., and Yamagata, T. (2013). Multiple causes of interannual sea surface temperature variability in the equatorial Atlantic Ocean. Nat. Geosci. 643. doi: 10.1038/ngeo1660

Richter, I., Xie, S. P., Behera, S. K., Doi, T., and Masumoto, Y. (2014a). Equatorial Atlantic variability and its relation to mean state biases in CMIP5. Clim. Dynam. 42, 171–188. doi: 10.1007/s00382-012-1624-5

Richter, I., Behera, S. K., Doi, T., Taguchi, B., Masumoto, Y., and Xie, S. P. (2014b). What controls equatorial Atlantic winds in boreal spring? Clim. Dyn. 43, 3091–3104. doi: 10.1007/s00382-014-2170-0

Richter, I. (2015). Climate model biases in the eastern tropical oceans: causes, impacts and ways forward. WIREs Clim. Change 6, 345–358. doi: 10.1002/wcc.338

Richter, I., and Coauthors, 2016: An overview of coupled GCM biases in the tropics. Indo-Pacific Climate Variability and Predictability, T. Yamagata and S. K. Behera, Eds., World Scientific Series on Asia-Pacific Weather and Climate, Vol. 8, World Scientific, 213–263, https://doi.org/10.1142/9789814696623_0008.

Richter, I., S.-P. Xie, Y. Morioka, T. Doi, B. Taguchi, and S. K. Behera, 2017: Phase locking of equatorial Atlantic variability through the seasonal migration of the ITCZ. *Climate Dyn.*, **48**, 3615–3629, https://doi.org/10.1007/s00382-016-3289-y.

Richter, I., Doi, T., Behera, S. K., and Keenlyside, N. (2018). On the link between mean state biases and prediction skill in the tropics: an atmospheric perspective. Clim. Dynam. 50, 3355–3374. doi: 10.1007/s00382-017-3809-4

Richter, I. and T. Doi, 2019: Estimating the Role of SST in Atmospheric Surface Wind Variability over the Tropical Atlantic and Pacific. J. Climate, 32, 3899–3915, https://doi.org/10.1175/JCLI-D-18-0468.1

Richter, I., and H. Tokinaga, 2020: An overview of the performance of CMIP6 models in the tropical Atlantic: mean state, variability, and remote impacts. *Clim. Dyn.*, under review

Rodríguez-Fonseca, B., Polo, I., García-Serrano, J., Losada, T., Mohino, E., Mechoso, C. R., et al. (2009). Are Atlantic Niños enhancing Pacific ENSO events in recent decades? Geophys. Res. Lett. 36:20705.

Rodríguez-Fonseca, B., and Coauthors, 2015: Variability and predictability of West African droughts: A review of the role of sea surface temperature anomalies. J. Climate, 28, 4034–4060, doi:https://doi.org/10.1175/JCLI-D-14-00130.1.

Rodwell, MJ, Rowell, DP, Folland, CK. 1999. Oceanic forcing of the winter North Atlantic Oscillation and European climate. Nature 398: 320– 323.

Rowell, D. P., C. K. Folland, K. Maskel, J. A. Owen, and M. N. Ward (1995), Variability of the summer rainfall over tropical North Africa (1906–92): Observations and modeling, Q. J. R. Meteorol. Soc., 121, 669–704, doi:10.1002/qj.49712152311.

Rowell, D. P., 2013: Simulating SST teleconnections to Africa: What is the state of the art? J. Climate, 26, 5397–5418, doi:10.1175/ JCLI-D-12-00761.1.

Ruiz-Barradas, A., J. A. Carton, and S. Nigam, 2000: Structure of interannual-to-decadal climate variability in the tropical Atlantic sector. *J. Climate*, **13,** 3285–3297.

Sasaki, W., T. Doi, K. J. Richards, and Y. Masumoto, 2015: The influence of ENSO on the equatorial Atlantic precipitation through the Walker circulation in a CGCM. Climate Dyn., 44, 191–202, doi:https://doi.org/10.1007/s00382-014-2133-5.

Scaife, A.A., Comer, R.E., Dunstone, N.J., Knight, J.R., Smith, D.M., MacLachlan, C., Martin, N., Peterson, K.A., Rowlands, D., Carroll, E.B., Belcher, S. and Slingo, J. (2017) Tropical rainfall, Rossby waves and regional winter climate predictions. Quarterly Journal of the Royal Meteorological Society, 143, 1– 11.

Servain, J., I. Wainer, J. P. McCreary, and A. Dessier, 1999: Relationship between the Equatorial and meridional modes of climatic variability in the tropical Atlantic. *Geophys. Res. Lett.*, **26,** 485–488.

Servain, J., Caniaux, G., Kouadio, Y. K., McPhaden, M. J., & Araujo, M. (2014). Recent climatic trends in the tropical Atlantic. Climate Dynamics, 43, 3071–3089. https://doi.org/10.1007/s00382-014-2168-7

Shannon, L. V., A. J. Boyd, G. B. Bundrit, and J. Taunton-Clark, 1986: On the existence of an El Niño-type phenomenon in the Benguela system. *J. Mar. Sci.*, **44,** 495–520.

Small, R. J., E. Curchitser, K. Hedstrom, B. Kauffman, and W. Large, 2015: The Benguela upwelling system: Quantifying the sensitivity to resolution and coastal wind representation in a global climate model. *J. Climate*, **28**, 9409–9432, doi:https://doi.org/10.1175/JCLI-D-15-0192.1.

Song, Z., Lee, S.-K., Wang, C., Kirtman, B., & Qiao, F. (2015). Contributions of the atmosphere–land and ocean–sea ice model components to the tropical Atlantic SST bias in CESM1. Ocean Modelling, 96, 280–290. https://doi.org/10.1016/j.ocemod.2015.09.008

Steinig, S., Harlaß, J., Park, W. & Latif, M. Sahel rainfall strength and onset improvements due to more realistic Atlantic cold tongue development in a climate model. *Scientific Reports* **8**, 1–9 (2018).

Stockdale TN, Balmaseda MA, Vidard A (2006) Tropical Atlantic SST prediction with coupled ocean-atmosphere GCMs. J Clim 19:6047–6061

Svendsen, L., N. G. Kvamstø, and N. S. Keenlyside, 2014: Weakening AMOC connects equatorial Atlantic and Pacific interannual variability. Climate Dyn., 43, 2931–2941, https://doi.org/ 10.1007/s00382-013-1904-8.

Tierney, J. E., N. J. Abram, K. J. Anchukaitis, M. N. Evans, C. Giry, K. H. Kilbourne, C. P. Saenger, H. C. Wu, and J. Zinke, 2015: Tropical sea surface temperatures for the past four centuries reconstructed from coral archives. *Paleoceanography*, **30,** 226-252.

Tokinaga, H., and S.-P. Xie, 2011b: Weakening of the equatorial Atlantic cold tongue over the past six decades. *Nat. Geosci.*, **4**, 222–226.

Tokinaga, H., I. Richter, and Y. Kosaka, 2019: ENSO Influence on the Atlantic Niño, Revisited: Multi-Year versus Single-Year ENSO Events. J. Climate, 32, 4585–4600, https://doi.org/10.1175/JCLI-D-18-0683.1

Tompkins, A. M., and L. Feudale, 2010: Seasonal ensemble predictions of West African monsoon precipitation in the ECMWF System 3 with a focus on the AMMA special observing period in 2006. *Wea. Forecasting*, **25**, 768–788.

Tseng, L., and C. R. Mechoso, 2001: A quasi-biennial oscillation in the equatorial Atlantic Ocean. *Geophys. Res. Lett.*, **28,** 187–190.

Venzke, S., M. R. Allen, R. T. Sutton, and D. P. Rowell, 1999: The atmospheric response over the North Atlantic to decadal changes in sea surface temperature. *J. Climate,* **12,** 2562–2584.

Wagner, R. G., and A. M. da Silva, 1994: Surface conditions associated with anomalous rainfall in the Guinea coastal region. Int. J. Climatol., 14, 179–199, doi:10.1002/joc.3370140205.

Wahl S, Latif M, Park W, Keenlyside N (2011) On the tropical atlantic SST warm bias in the Kiel climate model. Clim Dyn 36:891–906

Wittenberg, A. T., 2009: Are historical records sufficient to constrain ENSO simulations? *Geophys. Res. Lett.*, **36**, L12702, doi:10.1029/2009GL038710.

Xie, S-P., and S. G. H. Philander, 1994: A coupled ocean-atmosphere model of relevance to the ITCZ in the eastern Pacific. *Tellus*, **46A,** 340–350.

Xu, Z., Li, M., Patricola, C. M., & Chang, P. (2014a). Oceanic origin of southeast tropical Atlantic biases. Climate Dynamics, 43, 2915–2930. https://doi.org/10.1007/ s00382-013-1901-y

Xu, Z., Chang, P., Richter, I., & Kim, W. (2014b). Diagnosing southeast tropical Atlantic SST and ocean circulation biases in the CMIP5 ensemble. Climate Dynamics, 43, 3123–3145. https://doi.org/10.1007/s00382-014-2247-9

Zebiak, S. E., 1993: Air–sea interaction in the equatorial Atlantic region. *J. Climate*, **6**, 1567–1586.

Zermeno-Diaz, D., and C. Zhang, 2013: Possible root causes of surface westerly biases over the equatorial Atlantic in global climate models. J. Climate, 26, 8154–8168, doi:https://doi.org/10.1175/JCLI-D-12-00226.1.

Zhang, H., A. Clement, and P. Di Nezio, 2014: The South Pacific meridional mode: A mechanism for ENSO-like variability. J. Climate, 27, 769–783, https://doi.org/10.1175/JCLI-D-13-00082.1.

Zuidema, P., and Coauthors, 2016: Challenges and prospects for reducing coupled climate model SST biases in the eastern tropical Atlantic and Pacific Oceans: The U.S. CLIVAR eastern tropical oceans synthesis working group. Bull. Amer. Meteor. Soc., 97, 2305–2328, doi:https://doi.org/10.1175/BAMS-D-15-00274.1.

Captions

Table 1. Definition of averaging areas used in this study.

Figure 1. Climatological SST (color shading; ˚C), 10-m wind vectors (m s-1) and precipitation (blue shading; mm d-1) for 1979-2017. (a) MAM and (b) JJA seasons. SST and near-surface winds are from ERA5, precipitation from GPCP.

Figure 2. Climatological ERA5 SST (blue) and 10-m zonal wind (red) averaged over the ATL3 (solid line) and ATL4 (dashed line) regions, as a function of calendar month.

Figure 3. ITCZ latitude (green line; calculated as the latitude of maximum GPCP precipitation averaged between 45-20W) and ERA5 surface zonal wind averaged over the ATL4 region (blue line; m s-1). The winds have been multiplied by a factor -1 to facilitate comparison.

Figure 4. ERA5 climatological SLP (black line) and surface zonal wind (green dashed line) along the equator, averaged over March-April-May (MAM) and from 3ºS to 3ºN.

Figure 5. Equatorial vertical sections of climatological mass stream function (top; contours in 3 x 10^9 kg s-1 intervals; zero contour thickened), 10-m zonal wind (middle; m s-1 with westerly vectors in red and easterly in blue), and ocean subsurface temperature (bottom; color in ˚C). (a) MAM and (b) JJA. Black lines on the bottom panels indicate the climatological thermocline depth, defined by the maximum of vertical temperature gradient. All fields are derived from ERA5.

Figure 6. Time series of NCEP Reanalysis SST anomalies (K) averaged over the ATL3 region for the period 1949-2018. Linear detrending and 3-month running mean have been applied.

Figure 7. February to July composite anomalies of SST (shading; ˚C), 10-m wind (vector; m s-1), and precipitation (green contours at 1, 2, 3 mm day-1, and red contours at -1, -2, -3 mm day-1) for positive AZM events (Atlantic Niños). Data are from ERA5 (SST and 10-m wind) and GPCP (precipitation). The compositing criterion is based on the JJA mean ATL3 SST exceeding 0.75 standard deviations. The years 1984, 1988, 1991, 1995, 1996, 1999, 2007 and 2008 are selected. The years 1987, 1998, 2006 and 2010 also meet the criterion but are rejected due to being non-canonical (see section 4.6).

Figure 8. As in Fig.7, but for negative AZM events. The years 1982, 1983, 1992, 1997, 2004, 2005 and 2015 are selected for the composite.

Figure 9. Equatorial vertical sections of positive AZM composite anomalies from February to July. Zonal wind (top; contours in 0.5 m s-1 intervals; zero contour thickened), pressure velocity (top; color in 0.01 Pa s-1), 10-m zonal wind (middle; m s-1 with westerly vectors in red and easterly in blue), and ocean subsurface temperature (bottom; color in ˚C). Green and red lines on the bottom panels indicate the climatological and composite thermocline depth, respectively. Atmospheric data are from ERA5, oceanic data from ORAS4.

Figure 10. As in Fig. 9 but for negative AZM events.

Figure 11. Scatter plot of SST vs. surface zonal wind in the equatorial Pacific and Atlantic. The indices plotted are (a) JJA surface zonal wind anomalies averaged over the Niño 4 region vs. DJF SST anomalies averaged over the Niño 3 region, and (b) MAM surface zonal wind anomalies averaged over the ATL4 region vs. JJA SST anomalies averaged over the ATL3 region. The correlation coefficient between wind and SST is noted in the lower right.

Figure 12. ERA5 Surface zonal wind stress (N/m2; averaged 3ºS-3ºN) plotted as a function of Atlantic ITCZ latitude, here defined as the latitude where the zonal average of precipitation, averaged from 40ºW to 20ºW, attains its maximum. Surface zonal wind stress and precipitation are from ERA5 and GPCP, respectively (black line), and from the CMIP5 ensemble (blue line). The thin blue lines indicate the standard deviation of the inter-ensemble spread.

Figure 13. Anomalies of SST (shading; K) and near-surface winds (vectors; reference 0.5 m s-1) from the first mode of a maximum covariance analysis (MCA) for MAM. The MCA was calculated from linearly detrended ERA5 data. The pattern depicts the positive phase of the Atlantic Meridional Mode (AMM).

Figure 14. Latitude-time sections of CMIP5 ensemble mean biases of SST (shading; K), surface winds (vectors; reference = 2 m/s), and depth of the 20ºC isotherm (D20; purple contour lines; interval = 4 m), averaged between 3S-3N. The reference fields are ERA5 (SST and surface winds), and ORAS4 (D20).

Figure 15. Climatological annual cycle of the standard deviation of ATL3 SST (K) in ERA5 (black line) and the CMIP5 ensemble (green line).

Figure 16. Climatological annual cycle of (a) ATL3 SST (ºC), and (b) ATL4 sfc zonal wind. The black and green lines denote ERA5 and the CMIP5 ensemble, respectively.

A. Tables

area name	definition	use
ATL3	20ºW-0, 3ºS-3ºN	area of maximum SST variability; primary index of AZM
ATL4	45º-20ºW, 3ºS-3ºN	area of maximum surface zonal wind variability; equatorial Atlantic SST gradient (by taking the difference ATL4 minus ATL3)
Niño 3	150-90ºW, 5ºS-5ºN	measure of ENSO SST variability
Niño 4	160ºE-150ºW, 5ºS-5ºN	measure of ENSO surface zonal wind variability

Table 1. Definition of averaging areas used in this study.

B. Figures

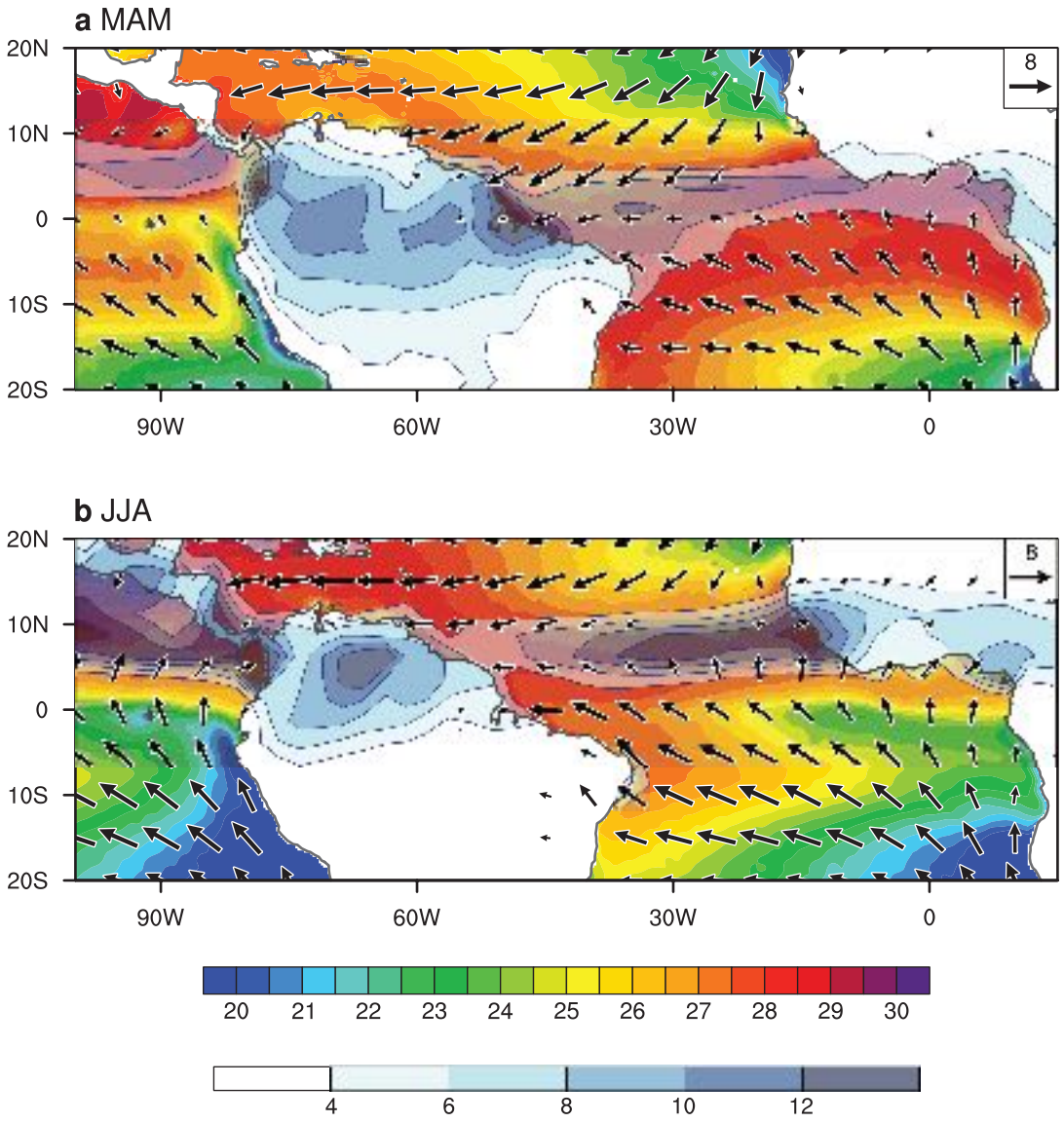

Figure 1. Climatological SST (color shading; ˚C), 10-m wind vectors (m s-1) and precipitation (blue shading; mm d^{-1}) for 1979-2017. (a) MAM and (b) JJA seasons. SST and near-surface winds are from ERA5, precipitation from GPCP.

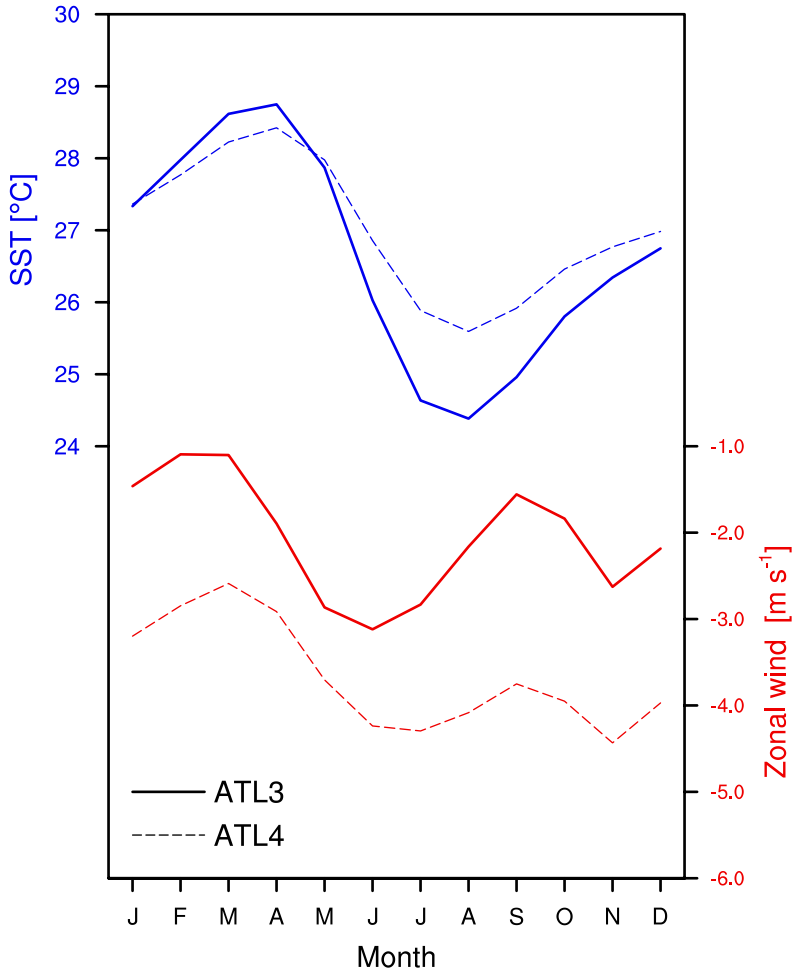

Figure 2. Climatological ERA5 SST (blue) and 10-m zonal wind (red) averaged over the ATL3 (solid line) and ATL4 (dashed line) regions, as a function of calendar month.

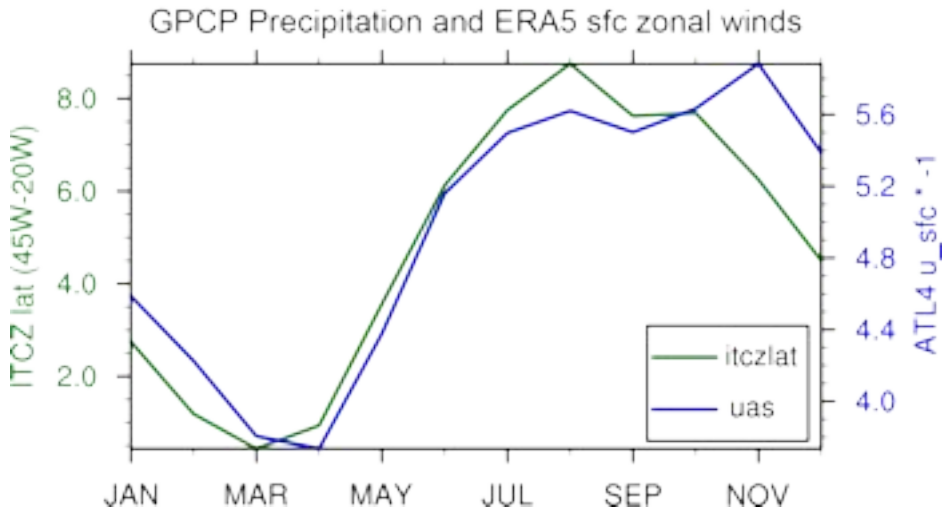

Figure 3. ITCZ latitude (degrees north; green line; calculated as the latitude of maximum GPCP precipitation averaged between 45-20W) and ERA5 surface zonal wind averaged over the ATL4 region (blue line; m s^{-1}). The winds have been multiplied by a factor -1 to facilitate comparison.

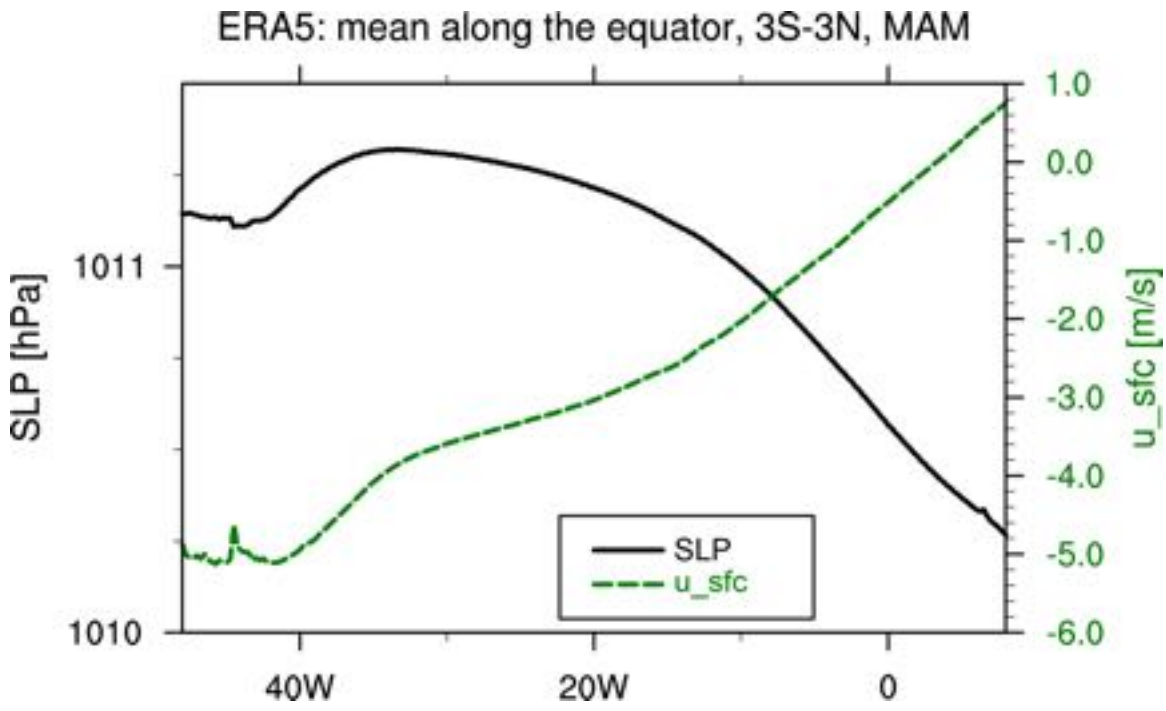

Figure 4. ERA5 climatological SLP (black line) and surface zonal wind (green dashed line) along the equator, averaged over March-April-May (MAM) and from 3ºS to 3ºN.

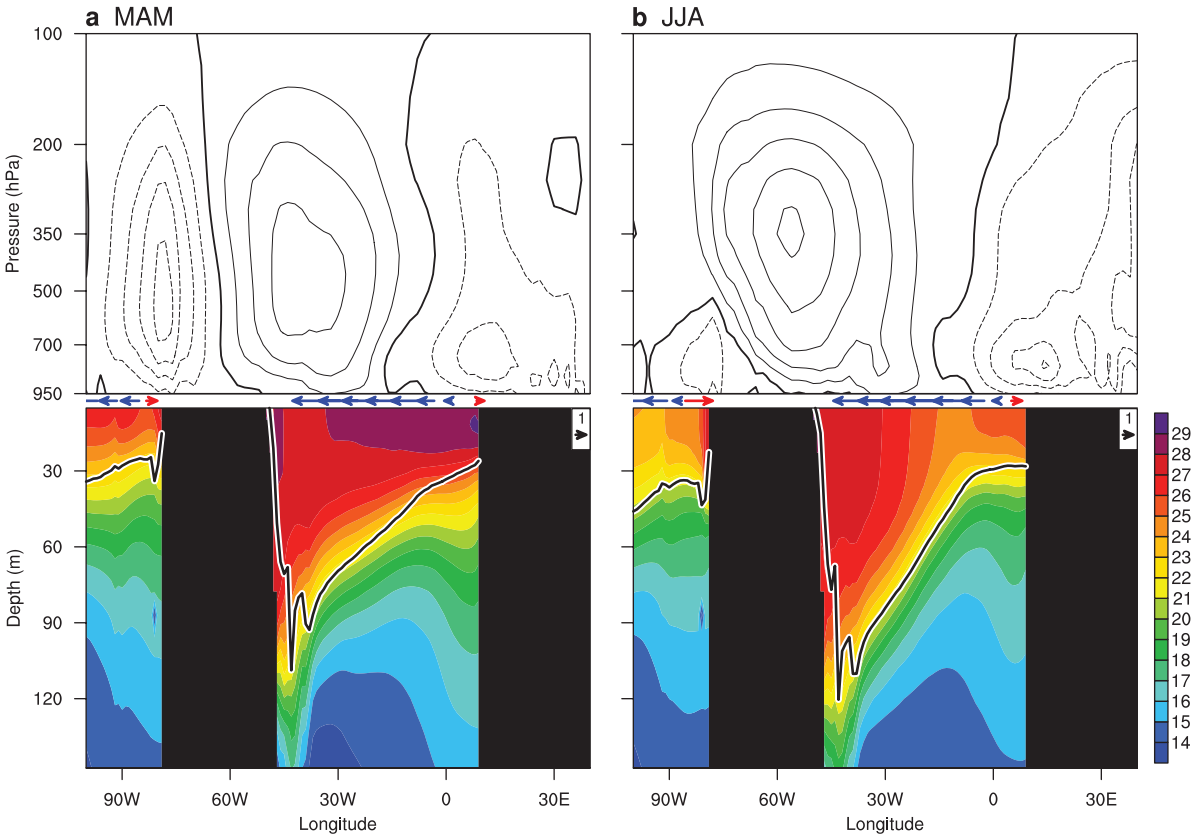

Figure 5. Equatorial vertical sections of climatological mass stream function (top; contours in 3 x 10^9 kg s^{-1} intervals; zero contour thickened), 10-m zonal wind (middle; m s^{-1} with westerly vectors in red and easterly in blue), and ocean subsurface temperature (bottom; color in ˚C). (a) MAM and (b) JJA. Black lines on the bottom panels indicate the climatological thermocline depth, defined by the maximum of vertical temperature gradient. All fields are derived from ERA5.

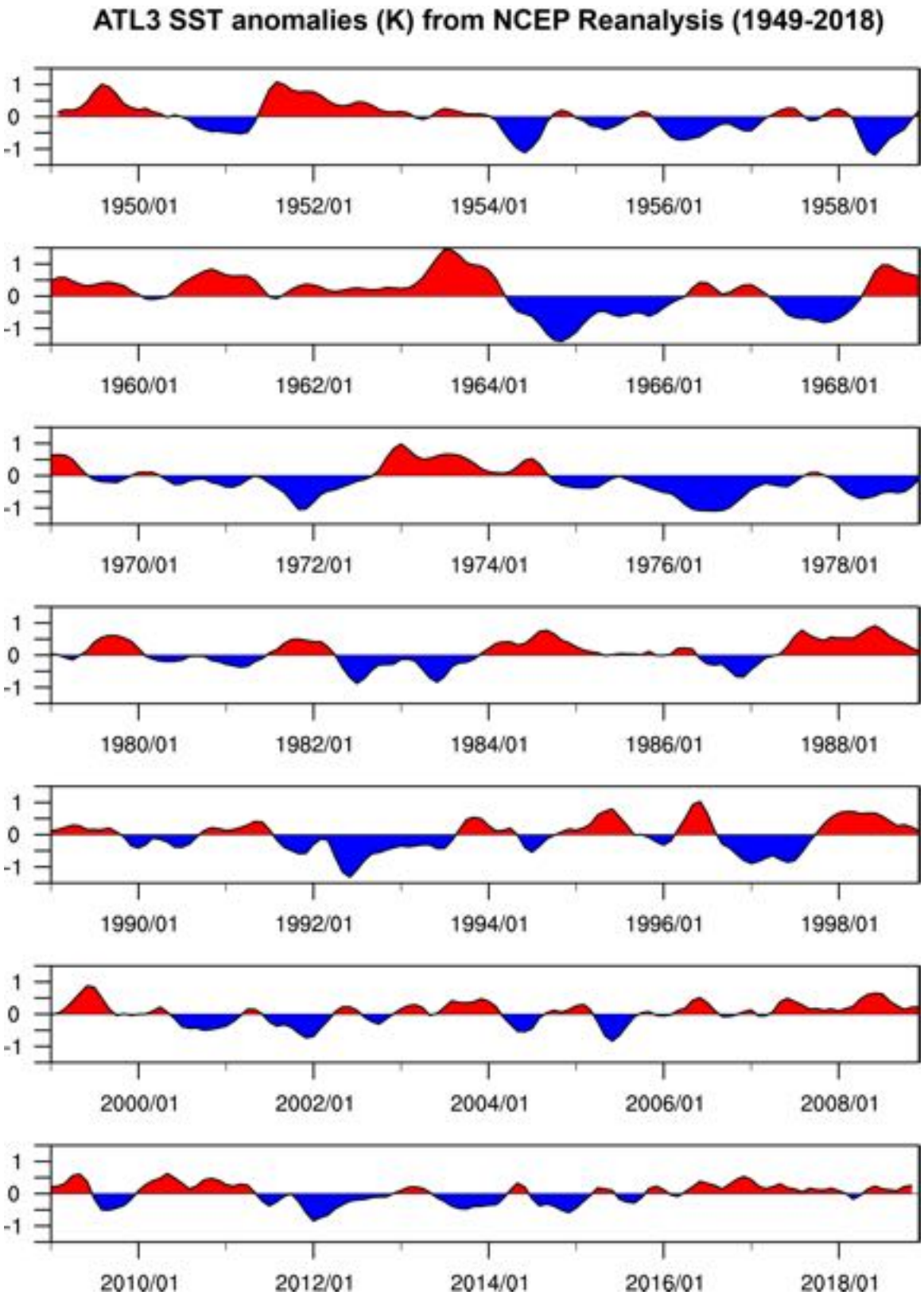

Figure 6. Time series of NCEP Reanalysis SST anomalies (K) averaged over the ATL3 region for the period 1949-2018. Linear detrending and 3-month running mean have been applied.

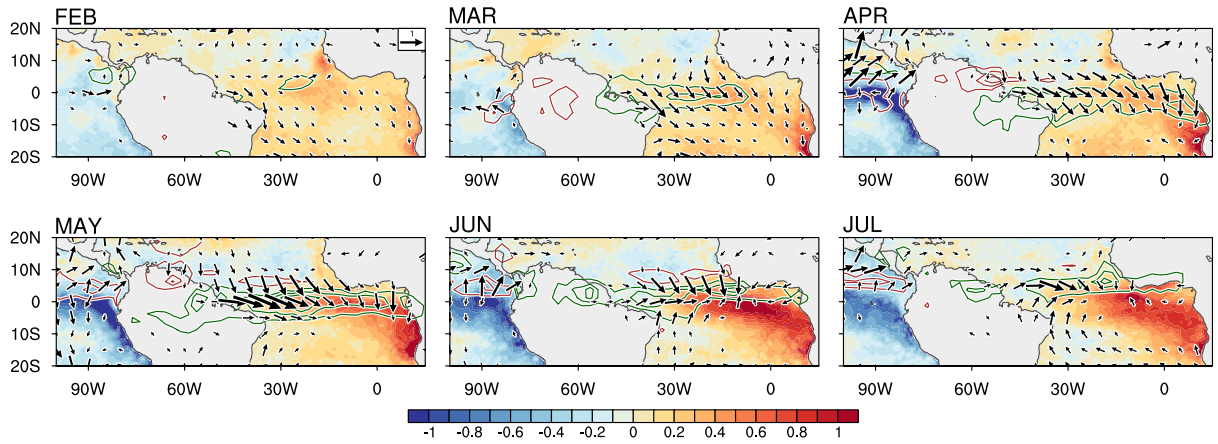

Figure 7. February to July composite anomalies of SST (shading; ˚C), 10-m wind (vector; m s^{-1}), and precipitation (green contours at 1, 2, 3 mm day^{-1}, and red contours at -1, -2, -3 mm day^{-1}) for positive AZM events (Atlantic Niños). Data are from ERA5 (SST and 10-m wind) and GPCP (precipitation). The compositing criterion is based on the JJA mean ATL3 SST exceeding 0.75 standard deviations. The years 1984, 1988, 1991, 1995, 1996, 1999, 2007 and 2008 are selected. The years 1987, 1998, 2006 and 2010 also meet the criterion but are rejected due to being non-canonical (see section 4.6).

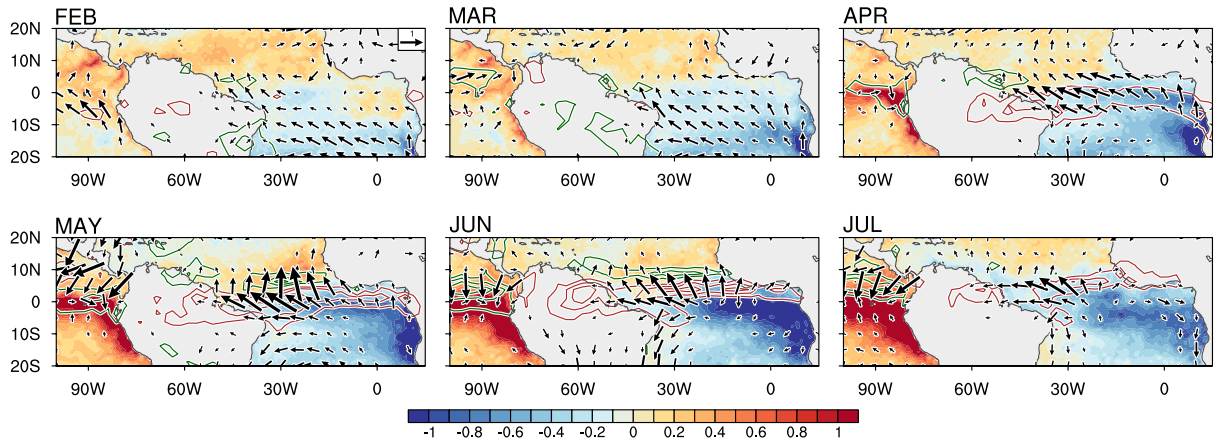

Figure 8. As in Fig.7, but for negative AZM events. The years 1982, 1983, 1992, 1997, 2004, 2005 and 2015 are selected for the composite.

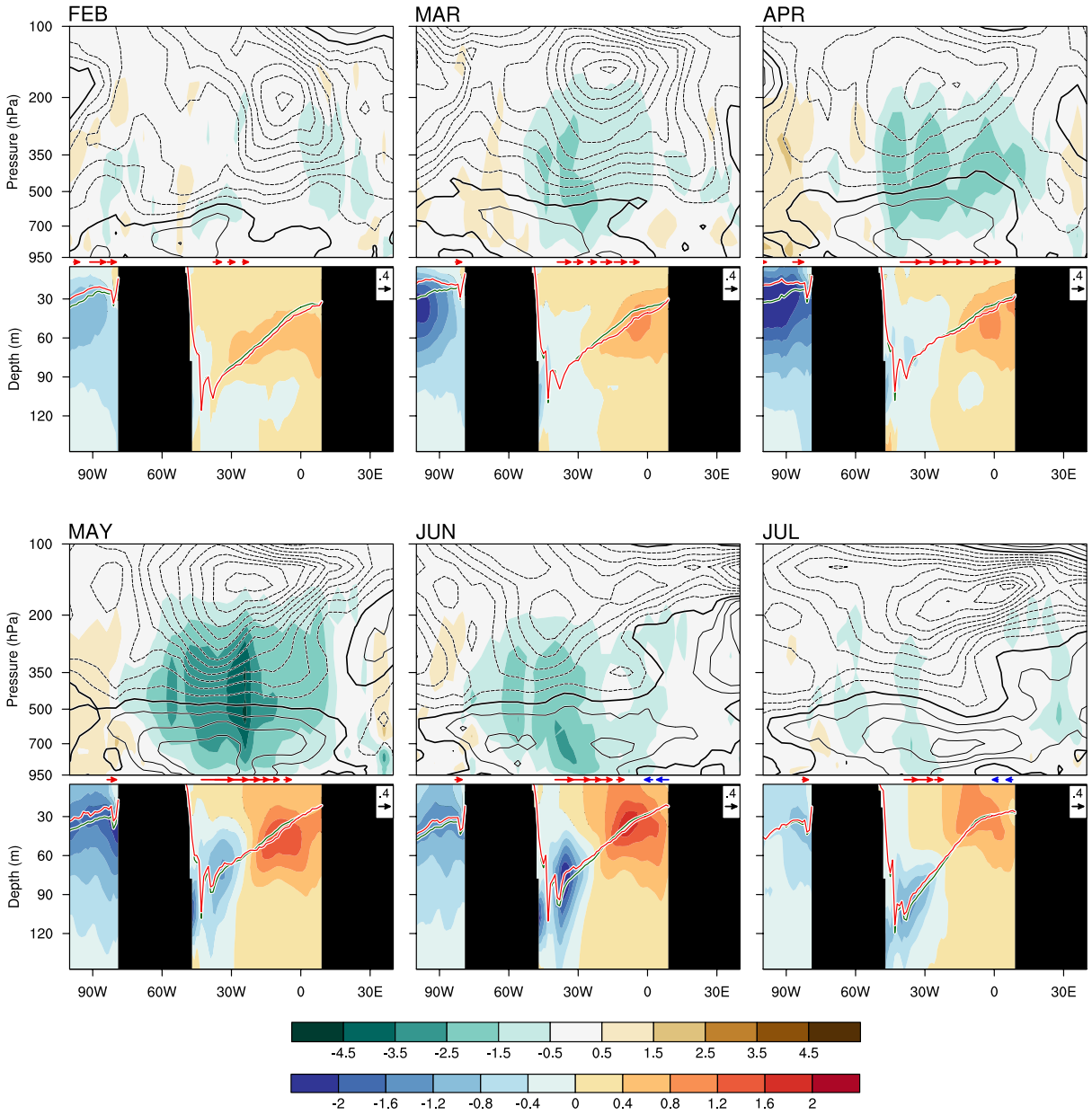

Figure 9. Equatorial vertical sections of positive AZM composite anomalies from February to July. Zonal wind (top; contours in 0.5 m s^{-1} intervals; zero contour thickened), pressure velocity (top; color in 0.01 Pa s^{-1}), 10-m zonal wind (middle; m s^{-1} with westerly vectors in red and easterly in blue), and ocean subsurface temperature (bottom; color in ˚C). Green and red lines on the bottom panels indicate the climatological and composite thermocline depth, respectively. Atmospheric data are from ERA5, oceanic data from ORAS4.

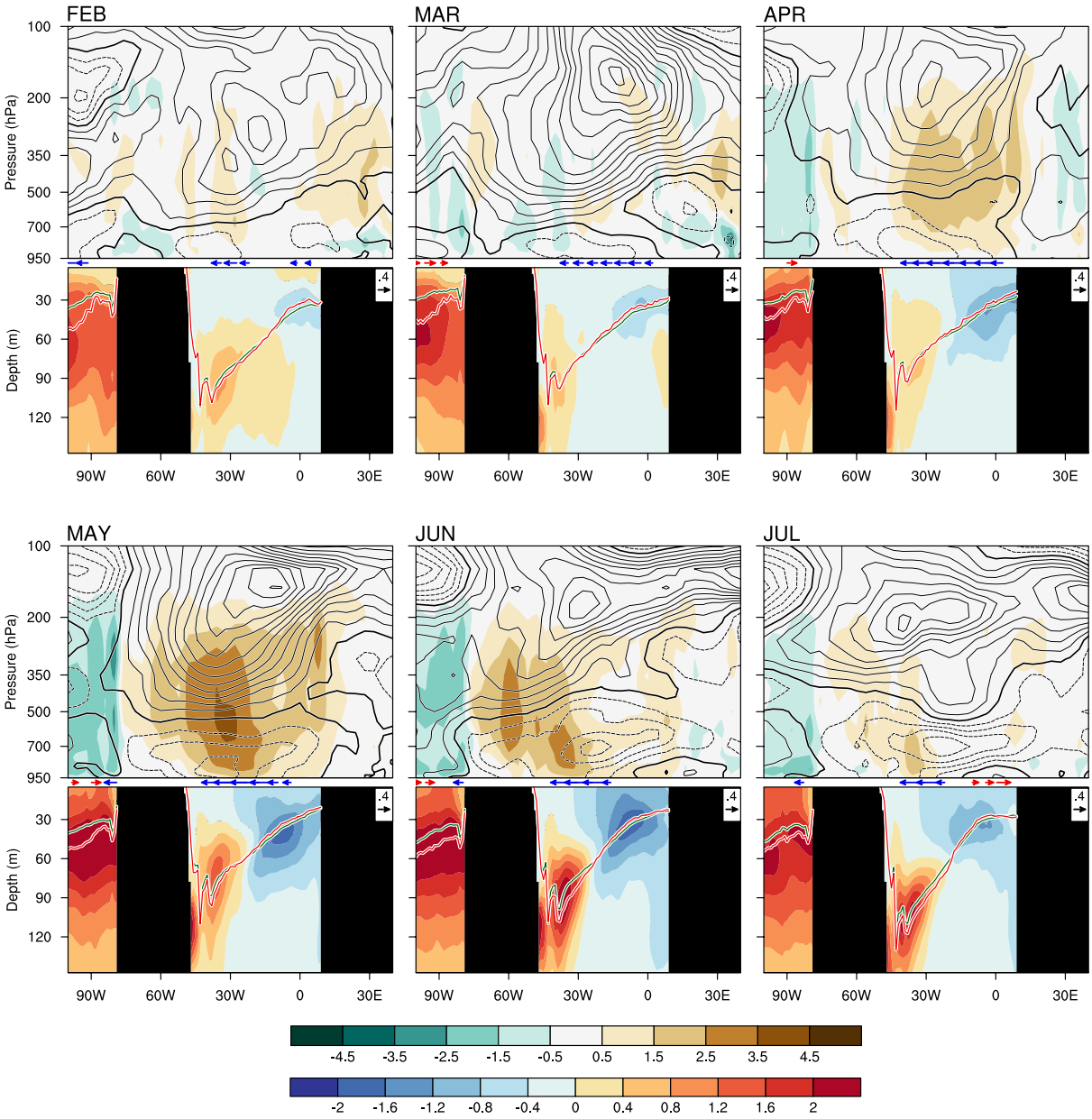

Figure 10. As in Fig. 9 but for negative AZM events.

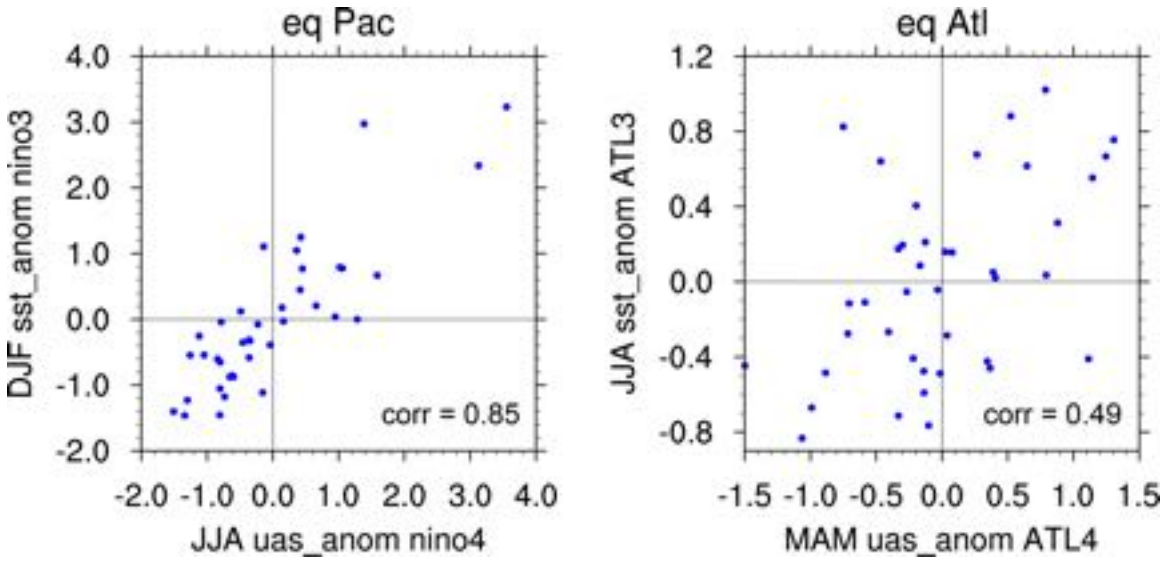

Figure 11. Scatter plot of SST vs. surface zonal wind in the equatorial Pacific and Atlantic. The indices plotted are (a) JJA surface zonal wind anomalies averaged over the Niño 4 region vs. DJF SST anomalies averaged over the Niño 3 region, and (b) MAM surface zonal wind anomalies averaged over the ATL4 region vs. JJA SST anomalies averaged over the ATL3 region. The correlation coefficient between wind and SST is noted in the lower right.

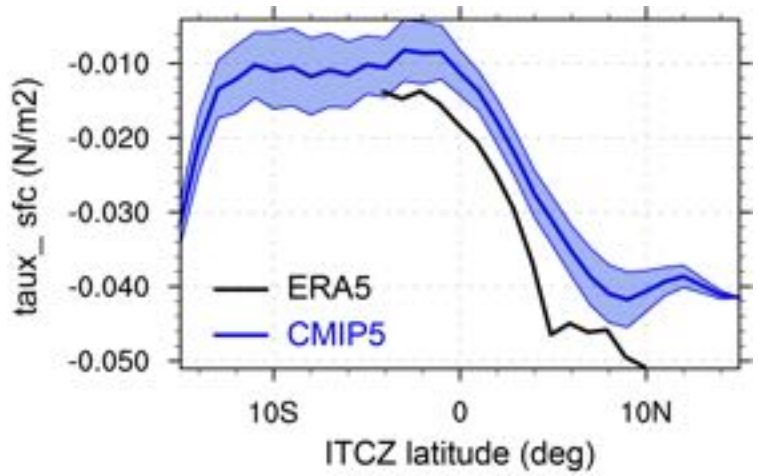

Figure 12. ERA5 Surface zonal wind stress (N/m^2; averaged 3ºS-3ºN) plotted as a function of Atlantic ITCZ latitude, here defined as the latitude where the zonal average of precipitation, averaged from 40ºW to 20ºW, attains its maximum. Surface zonal wind stress and precipitation are from ERA5 and GPCP, respectively (black line), and from the CMIP5 ensemble (blue line). The thin blue lines indicate the standard deviation of the inter-ensemble spread.

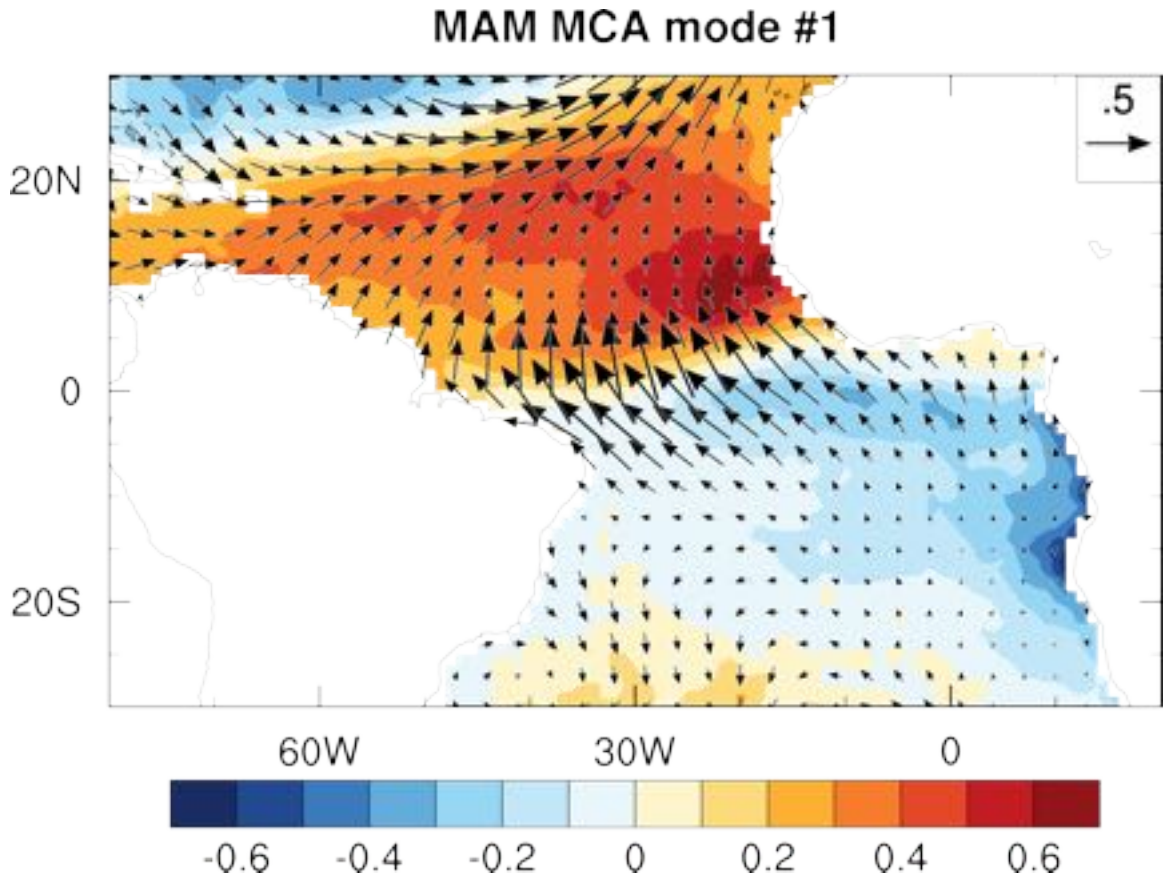

Figure 13. Anomalies of SST (shading; K) and near-surface winds (vectors; reference 0.5 m s^{-1}) from the first mode of a maximum covariance analysis (MCA) for MAM. The MCA was calculated from linearly detrended ERA5 data. The pattern depicts the positive phase of the Atlantic Meridional Mode (AMM).

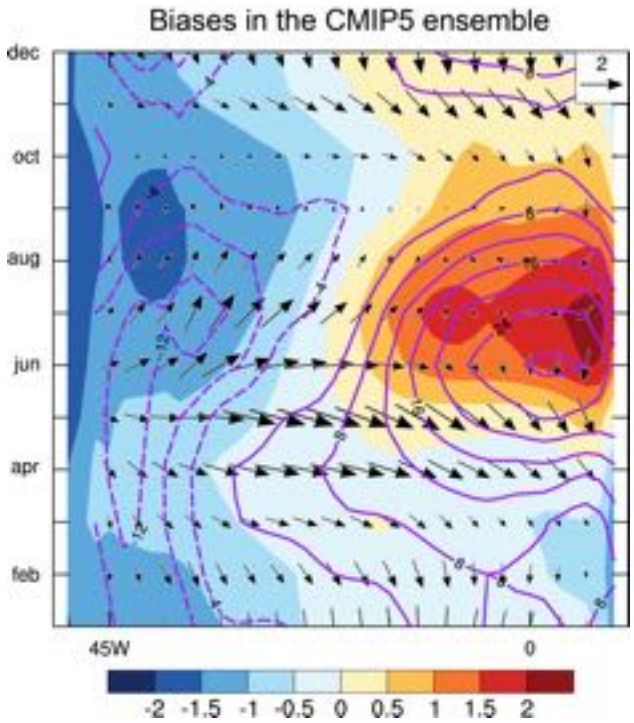

Figure 14. Latitude-time sections of CMIP5 ensemble mean biases of SST (shading; K), surface winds (vectors; reference = 2 m/s), and depth of the 20ºC isotherm (D20; purple contour lines; interval = 4 m), averaged between 3S-3N. The reference fields are ERA5 (SST and surface winds), and ORAS4 (D20).

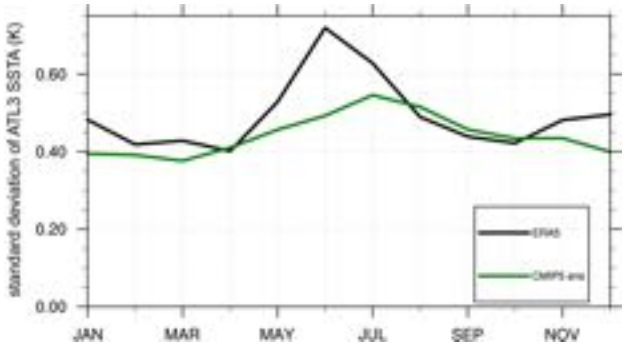

Figure 15. Climatological annual cycle of the standard deviation of ATL3 SST (K) in ERA5 (black line) and the CMIP5 ensemble (green line).

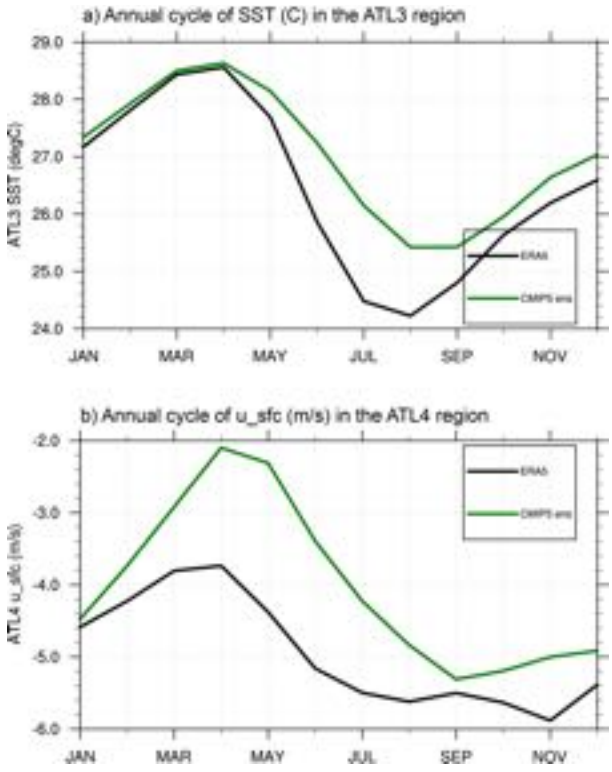

Figure 16. Climatological annual cycle of (a) ATL3 SST (ºC), and (b) ATL4 surface zonal wind. The black and green lines denote ERA5 and the CMIP5 ensemble, respectively.